J Pharmacokinet Pharmacodyn (2010) 37:365–405
DOI 10.1007/s10928-010-9165-1

Lumping of physiologically-based pharmacokinetic models and a mechanistic derivation of classical compartmental models

Sabine Pilari · Wilhelm Huisinga

Received: 4 June 2010 / Accepted: 9 July 2010 / Published online: 27 July 2010

Abstract In drug discovery and development, classical compartment models and physiologically based pharmacokinetic (PBPK) models are successfully used to analyze and predict the pharmacokinetics of drugs. So far, however, both approaches are used exclusively or in parallel, with little to no cross-fertilization. An approach that directly links classical compartment and PBPK models is highly desirable. We derived a new mechanistic lumping approach for reducing the complexity of PBPK models and establishing a direct link to classical compartment models. The proposed method has several advantages over existing methods: Perfusion and permeability rate limited models can be lumped; the lumped model allows for predicting the original organ concentrations; and the volume of distribution at steady state is preserved by the lumping method. To inform classical compartmental model development, we introduced the concept of a minimal lumped model that allows for prediction of the venous plasma concentration with as few compartments as possible. The minimal lumped parameter values may serve as initial values for any subsequent parameter estimation process. Applying our lumping method to 25 diverse drugs, we identified characteristic features of lumped models for moderate-to-strong bases, weak bases and acids. We observed that for

S. Pilari
Department of Mathematics and Computer Science, Freie Universität, Berlin, Germany
e-mail: pilari@mi.fu-berlin.de

S. Pilari
Graduate Research Training Program PharMetrX: Pharmacometrics and Computational Disease Modeling, Martin- Luther- Universität Halle-Wittenberg and Freie Universität, Berlin, Germany

W. Huisinga (✉)
Hamilton Institute, National University of Ireland Maynooth (NUIM), Maynooth, Ireland
e-mail: wilhelm.huisinga@nuim.ie
URL: http://www.hamilton.ie/compphysiol

acids with high protein binding, the lumped model comprised only a single compartment. The proposed lumping approach established for the first time a direct derivation of simple compartment models from PBPK models and enables a mechanistic interpretation of classical compartment models.

Keywords Classical model · Compartment PK model · Physiologically based pharmacokinetics · PBPK · Mechanistic lumping · Volume of distribution · Minimal lumped model · Transfer of knowledge

Introduction

During preclinical and clinical drug development, a variety of in vitro and in vivo data are collected to investigate the pharmacokinetics (PK) and pharmacodynamics of a drug candidate, e.g., [1, 2]. A common approach to examine the PK of a drug is by classical compartmental analysis, e.g., [3, 4]. Usually, a low dimensional compartment model is fitted to in vivo plasma or blood data and then used to derive key characteristics (AUC, CL, tmax, Cmax etc.) or for extrapolation (different routes of administration, multiple dosing, allometric scaling). Another approach to investigate the PK of a drug is whole-body physiologically based pharmacokinetic (PBPK) modeling [5–9]. PBPK models represent relevant absorption, distribution, metabolism and excretion (ADME) processes in a mechanistic way and allow for the integration of diverse in vitro and in vivo data. PBPK models can be used to predict plasma concentration profiles prior to any in vivo studies, solely based on in vitro data. If gradually refined and evaluated against preclinical and early clinical data, a PBPK model can be seen as reflecting part of the current knowledge about a drug candidate, stated in the language of mathematics. Such models, however, are less suitable for estimation of individual parameters as part of, e.g., in population analysis of clinical trails [10] due to their complexity.

So far, the classical compartmental PK and the physiologically-based PK approach are used independently or in parallel, with little to no overlap or cross-fertilization. In particular, classical compartmental model development does not directly benefit from the knowledge that is present in a PBPK model. An approach that establishes the link between mechanistic PBPK models and classical compartmental models is therefore highly desirable.

The objective of this article is to translate prior knowledge on the PK of a compound given in form of a whole-body PBPK model into the development of classical compartmental models in different stages of the drug development process. For a given drug, we determine essential characteristics of PK compartment models by lumping of the detailed whole-body PBPK model. Our approach is based on a new lumping method that determines the number and composition of lumped compartments based on the PK profiles in the distribution and elimination phase.

In literature, several approaches for the reduction and lumping of PBPK models have been proposed [11–14]. These methods, however, rely on much more restrictive lumping rules that have difficulties to justify lumping a detailed PBPK model to, e.g., a 1- or 2-compartment model. Such low dimensional models,

however, are frequently used in all stages of the development process to describe clinical data, e.g., [10]. In addition, only the concentration of the lumped compartments are predicted by the existing lumping approaches, while no link to the drug concentration of the original organs and tissues is established (unless this tissue is left unlumped, as suggested in [12]).

Our proposed new lumping procedure overcomes these limitations. It exploits the fact that drug concentrations in different compartments of the whole-body PBPK model are often strongly kinetically dependent of each other. We quantify and exploit this dependence to establish the lumped model and to relate the lumped concentrations back to the original ones. Using parametrization of PBPK models based on recent methods to a priori predict tissue-partition coefficients [15–18], we observe characteristic features for moderate-to-strong bases, weak bases and acids. For acids with a low fraction unbound in plasma (fu^p), e.g., a 1-compartment model was sufficient to predict the concentration-time course of all 13 tissues and organs in the original PBPK model.

Material and methods

Generic PBPK model

A general introduction to PBPK modeling can be found, e.g., in [5–7, 9, 19–21]. Our detailed PBPK model comprised 13 compartments representing important tissues, organs or other spaces within the human body (see Fig. 1). The model accounts for the anatomical compartments arterial and venous blood, lung, adipose tissue, bone, brain, gut, heart, kidneys, liver, muscle, skin, and spleen. For simplicity, we used the subscript 'tis' to refer to tissues and organs.

As typically done in the generic setting and in the absence of more specific information, we assume that the drug distributes within the body via transport by the blood flow and via passive diffusion homogeneously into organs and tissues, and that the drug is metabolized in the liver. In the presence of more specific information, the generic PBPK model can be adapted accordingly, e.g., to account for active transport processes, excretion by the kidneys, specific protein binding, saturable metabolism etc.

Based on the perfusion-limited (well-stirred) tissue model, the following differential equation (ODE) describes the distribution processes in each non-eliminating organ/tissue:

$$V_{\text{tis}} \frac{\mathrm{d}}{\mathrm{dt}} C_{\text{tis}} = Q_{\text{tis}} \cdot \left(C_{\text{in}} - \frac{C_{\text{tis}}}{K_{\text{tis}}} \right), \tag{1}$$

where C_{tis} represents the total drug concentration in the organ/tissue and C_{in} represents the influent blood concentration. In most cases, this is the arterial blood concentration (see below for more details). V_{tis} and Q_{tis} denote the tissue volume and blood flow, respectively. The tissue-to-blood partition coefficient, K_{tis}, relates the steady state tissue drug concentration to the steady state blood concentration.

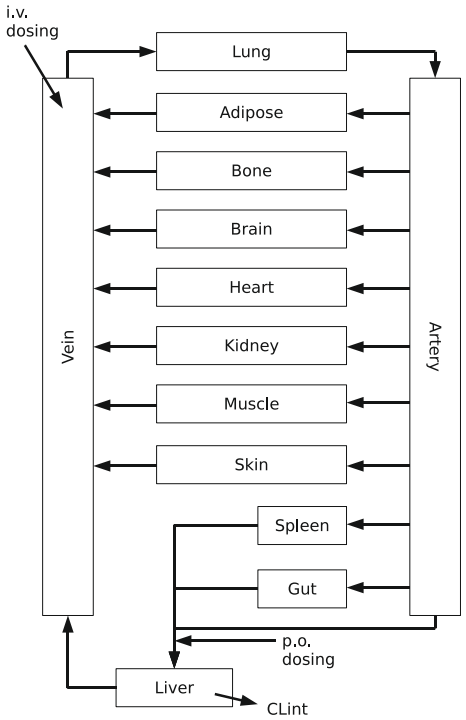

Fig. 1 Organ and tissue topology of the generic 13 compartment PBPK model. In the generic model, only hepatic elimination is assumed. If knowledge about further routes of elimination (e.g., renal) is available, this can easily be integrated

$$K_{\text{tis}} = \frac{C_{ss,\text{tis}}}{C_{ss,\text{blood}}}. \tag{2}$$

Thus, in Eq. 1, the term $C_{\text{tis}}/K_{\text{tis}}$ represents the blood concentration leaving the compartment. Since metabolism is assumed to occur in the liver, the corresponding ODE is:

$$V_{\text{liv}} \frac{\text{d}}{\text{dt}} C_{\text{liv}} = Q_{\text{liv}} \cdot \left(C_{\text{in}} - \frac{C_{\text{liv}}}{K_{\text{liv}}} \right) - \text{CL}_{\text{int}} C_{\text{liv}}, \tag{3}$$

where CL_{int} denotes the hepatic intrinsic clearance. Alternatively, some PBPK models assume that only the unbound concentration in the liver tissue $C_{\text{u,liv}}$ can be metabolized, resulting in a term $\text{CL}_{\text{int}} \cdot C_{\text{u,liv}}$ instead of $\text{CL}_{\text{int}} \cdot C_{\text{liv}}$. Assuming that $C_{\text{u,liv}} = \text{fu}_{\text{liv}} \cdot C_{\text{liv}}$, this can easily be integrated in our setting by changing CL_{int} to $\text{CL}_{\text{int}} \cdot \text{fu}_{\text{liv}}$.

For the artery and vein compartments the ODEs are

$$V_{\text{art}} \frac{\text{d}}{\text{dt}} C_{\text{art}} = Q_{\text{co}} \cdot (C_{\text{in}} - C_{\text{art}}), \tag{4}$$

$$V_{\text{ven}} \frac{\text{d}}{\text{dt}} C_{\text{ven}} = Q_{\text{co}} \cdot (C_{\text{in}} - C_{\text{ven}}), \tag{5}$$

where Q_{co} denotes the cardiac output. For all organs except lung, liver, artery and vein, it is $C_{\text{in}} = C_{\text{art}}$. For the lung, it is $C_{\text{in}} = C_{\text{ven}}$, and for the artery, it is

$C_{\text{in}} = C_{\text{lun}}$. The influent liver and venous blood concentrations are defined by the blood flow weighted sums of all organ concentrations that supply these compartments. For liver, it is

$$C_{\text{in}} = \frac{1}{Q_{\text{liv}}} \sum_{\text{tis}} Q_{\text{tis}} \frac{C_{\text{tis}}}{K_{\text{tis}}}, \tag{6}$$

where the sum is take of spleen, gut and the arterial hepatic vein. For the vein it is

$$C_{\text{in}} = \frac{1}{Q_{\text{co}}} \sum_{\text{tis}} Q_{\text{tis}} \frac{C_{\text{tis}}}{K_{\text{tis}}}, \tag{7}$$

where the sum is taken of adipose, bone, brain, heart, kidneys, muscle, skin and the liver.

Frequently used routes of drug administration are a bolus i.v. administration, an i.v. infusion and a p.o. administration. This requires to extend the venous blood and the liver ODE correspondingly. For a bolus i.v. administration, the initial condition $C(t = 0)$ for the system of ODEs is set to $C_{\text{ven}}(0) = \text{dose}/V_{\text{ven}}$, while all other initial concentrations are set to zero. For an i.v. infusion, the venous ODE has to be changed to:

$$V_{\text{ven}} \frac{\text{d}}{\text{dt}} C_{\text{ven}} = Q_{\text{ven}} \cdot (C_{\text{in}} - C_{\text{ven}}) + r_{\text{iv}}, \tag{8}$$

where 'r_{iv}' denotes the mass influx due to an i.v. infusion given by

$$r_{\text{iv}} = \begin{cases} \text{dose}/\Delta T; & t \in [T_0, T_0 + \Delta T] \\ 0; & \text{otherwise}, \end{cases} \tag{9}$$

with starting time T_0 and duration ΔT. In the case of p.o. drug administration, the liver ODE has to be amended to

$$V_{\text{liv}} \frac{\text{d}}{\text{dt}} C_{\text{liv}} = Q_{\text{liv}} \cdot \left(C_{\text{in}} - \frac{C_{\text{liv}}}{K_{\text{liv}}} \right) - \text{CL}_{\text{int}} C_{\text{liv}} + r_{\text{po}(\text{F}\cdot\text{G})}, \tag{10}$$

where '$r_{\text{po}(\text{F}\cdot\text{G})}$' denotes the mass influx due to a p.o. administration. For a first order absorption model it is:

$$r_{\text{po}(\text{F}\cdot\text{G})} = \text{dose} \cdot F_{\text{F}\cdot\text{G}} \cdot k_{\text{a}} \cdot e^{-k_{\text{a}} \cdot t}, \tag{11}$$

where k_{a} denotes the first order absorption rate constant and $F_{\text{F}\cdot\text{G}}$ denotes the product of the fraction absorbed F_{F} and fraction not metabolized in the gut $F_{\text{G}} = (1 - \text{E}_{\text{gut}})$. Using the hepatic extraction ratio E_{hep} (see Eq. 16 below), we have

$$F_{\text{bio}} = (1 - \text{E}_{\text{hep}}) \cdot \underbrace{(1 - \text{E}_{\text{gut}}) \cdot F_{\text{F}}}_{F_{\text{F}\cdot\text{G}}}, \tag{12}$$

where F_{bio} denotes the bioavailability of the compound. We define for later reference

$$r_{\mathrm{po}(\mathrm{F_{bio}})} = \mathrm{dose} \cdot F_{\mathrm{bio}} \cdot k_{\mathrm{a}} \cdot e^{-k_{\mathrm{a}} \cdot t}, \tag{13}$$

where the oral absorption model already accounts for hepatic extraction.

Parametrization

A whole-body PBPK model requires species-specific physiological and anatomical parameters in addition to drug-specific data. Tissue volumes per kg body weight and blood flows in % of cardiac output are given in Table 1. We consider the standard male human with a body weight of 73 kg and a cardiac output of 6.5 l/min [22, 23]. Physicochemical and pharmacokinetic data for a number of drugs from different classes are summarized in Table 3. We use the drug Lidocaine to demonstrate our general approach. It is commonly used as an antiarrythmic drug in the treatment of ventricular arrhythmias [3, 34]. Its organ-specific tissue-to-blood partition coefficients, K_{tis}, are listed in Table 1, right column. We determined K_{tis} from the tissue-to-unbound plasma partition coefficients, $K\mathrm{u}_{\mathrm{tis}}$, via the relation

$$K_{\mathrm{tis}} = \frac{\mathrm{fu^p}}{\mathrm{B{:}P}} K\mathrm{u}_{\mathrm{tis}}, \tag{14}$$

where $\mathrm{fu^p}$ and B:P are the fraction unbound in plasma and the blood-to-plasma ratio, respectively. We predicted $K\mathrm{u}_{\mathrm{tis}}$ based on the model proposed by Rodgers et al. [15–18] to a priori predict tissue-to-unbound plasma partition coefficients. The quality of the a priori methods to predict tissue-to-unbound drug partition coefficients is 84–89% (within factor 3 of experimental values, reported for the species rat) [15, 17]. Situations that can give rise to under- or over-predictions of $K\mathrm{u}_{\mathrm{tis}}$ values include active transport processes, non-linear pharmacokinetics and binding to tissue constituents not accommodated in the mechanistic equations. In addition, insufficiently long infusion times for the experimental determination of the tissue-to-unbound plasma partition coefficients result in deviations between in silico and in vivo values. Drug-specific input parameters are $\mathrm{fu^p}$, $\mathrm{pK_a}$, $\log P_{\mathrm{ow}}$ and potentially B:P.

While often the intrinsic clearance is used to model hepatic metabolism in whole-body PBPK models, clinical studies and associated PK compartment models use the hepatic blood clearance $\mathrm{CL_{blood}}$. Employing the widely-used well-stirred liver model, both are related according to

$$\mathrm{CL_{blood}} = \frac{Q_{\mathrm{liv}} \mathrm{CL_{int}} \mathrm{K_{liv}}}{Q_{\mathrm{liv}} + \mathrm{CL_{int}} K_{\mathrm{liv}}}, \tag{15}$$

where K_{liv} denotes the liver tissue-to-blood partition coefficient (e.g., as resulting from Eq. 14). The hepatic extraction ratio, $\mathrm{E_{hep}}$, is defined as

$$\mathrm{E_{hep}} = \frac{\mathrm{CL_{int}} \mathrm{K_{liv}}}{Q_{\mathrm{liv}} + \mathrm{CL_{int}} K_{\mathrm{liv}}}, \tag{16}$$

with $0 \leq \mathrm{E_{hep}} < 1$.

Given a PBPK model, the volume of distribution in steady state V_{ss} can be readily estimated by

Table 1 Organ-specific data of the human PBPK model

Tissue	Volume (l/kg BW)	Blood flow (fraction of CO)	K_{tis}
Artery	0.0257	1.00	–
Vein	0.0514	1.00	–
Adipose	0.1196	0.05	1.548
Bone	0.0856	0.05	1.940
Brain	0.0200	0.12	1.871
Gut	0.0171	0.17	3.780
Heart	0.0047	0.04	3.033
Kidney	0.0044	0.19	6.236
Liver	0.0257	0.25	5.923
Lung	0.0076	1.00	4.699
Muscle	0.4000	0.17	2.514
Skin	0.0371	0.05	2.175
Spleen	0.0026	0.02	4.144

The physiological data are taken from [6]. We consider the standard male human with a body weight of 73 kg and an cardiac output of 6.5 l/min [22, 23]. The right column shows the tissue-to-blood partition coefficients, K_{tis} (see Eq. 14) that are predicted based on the tissue-to-unbound plasma partition coefficients Ku^{tis} according to [15, 17] for Lidocaine. *BW* body weight, *CO* cardiac output

$$V_{ss} = V_{blood} + \sum_{tis} V_{tis} K_{tis} + V_{liv} K_{liv} (1 - E_{hep}), \tag{17}$$

where the sum $\sum_{tis}$ is taken over all non-eliminating tissues/organs of the detailed PBPK model.

Residual error measurements

We compared the predicted concentration for venous plasma based on the 13-compartment PBPK model (C_{PBPK}) and a lumped compartment model (C_{Lumped}) using the following measure of the residual error:

$$\left\| C_{PBPK} - C_{Lumped} \right\|_{PBPK} = \frac{\int_0^T |C_{PBPK}(t) - C_{Lumped}(t)| \, dt}{\int_0^T C_{PBPK}(t) \, dt}, \tag{18}$$

where T denotes the final simulation time. The denominator of the above measure is identical to the well-known area under the concentration-time curve $AUC_{0\text{-}T}$, so we measured the deviation between predictions relative to the $AUC_{0\text{-}T}$ as predicted by the PBPK model.

Simulations and model fitting

We used MATLAB R2009a, version 7.8 for modeling and simulation (ode15s solver). Model fitting was performed using the MATLAB Optimization Toolbox, version 4.2, and the predefined function 'lsqcurvefit' with default options and the sum of least squares deviation as the criterion for model discrimination.

Results

Lumping of whole-body PBPK models

The simulation results of the generic PBPK model for Lidocaine are shown in Fig. 2. As Lidocaine is typically injected as an antiarrhythmic drug [34], we considered a 60 min infusion of Lidocaine. Its therapeutic concentrations are within 2–6 mg/l [3], whereas no more than 600 mg should be given in any 12 hour period [34]. We chose a total dose of 400 mg Lidocaine so that after $\sim$10 min a blood concentration in the therapeutic window is reached (see Fig. 2, vein).

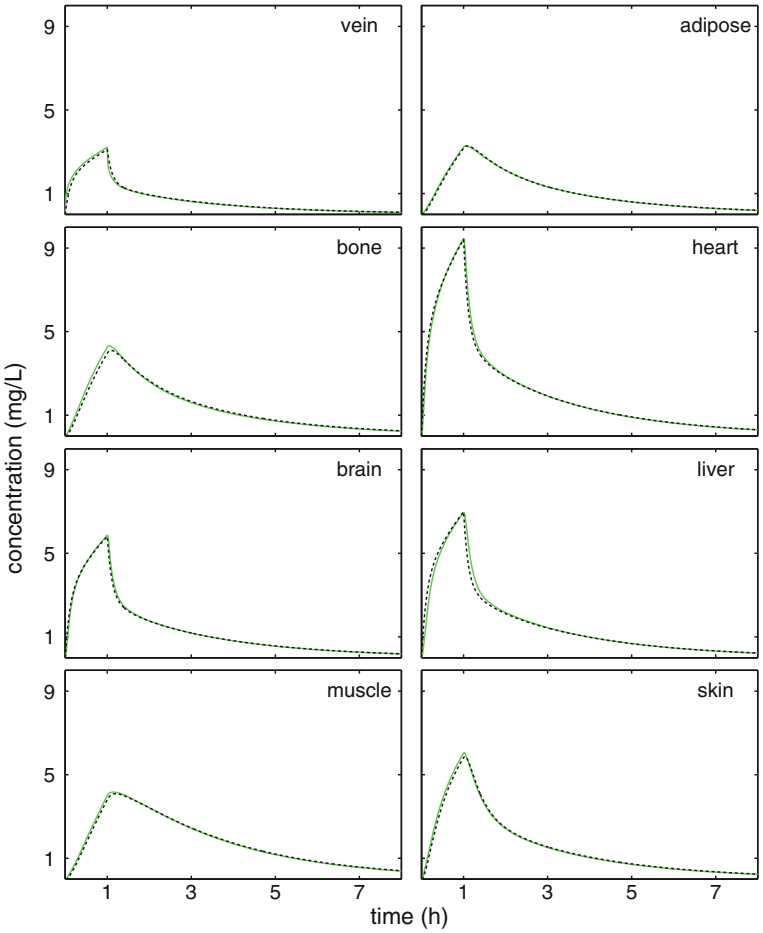

Fig. 2 Predictions of the 13 compartment whole-body PBPK model (*green solid line*), and the lumped 4-compartment PK model (*black dashed line*) following a 60 min infusion of 400 mg of Lidocaine in human for eight representative organs/tissues. The detailed PBPK model and the lumped model show excellent agreement. (Color figure online)

In the sequel, we describe the proposed lumping procedure. The input data were the concentration-time profiles in the different organs, tissues and other spaces as predicted by the whole-body PBPK model. In this study, we focussed on the important class of PBPK models, where all absorption, distribution, metabolism and excretion processes are non-saturable. We first dealt with perfusion rate-limited (well-stirred) organ models, while then we extended the lumping to permeability rate-limited organ models.

Identification of organs and tissues to be lumped together

Figure 3 (top) is the key to understand the new lumping method. It depicts *normalized* concentration-time profiles of all 13 compartments of the detailed PBPK model (for Lidocaine). Each concentration-time profile $C_{\text{tis}}(t)$ was normalized by its elimination-corrected tissue-to-blood partition coefficient, i.e.

$$\text{Normalized Concentration} = \frac{C_{\text{tis}}(t)}{K_{\text{tis}}(1 - E_{\text{tis}})}, \tag{19}$$

where for non-eliminating tissues, it is $E_{\text{tis}} = 0$, while for eliminating tissues E_{tis} denotes the tissue extraction ratio. In our PBPK model for Lidocaine, only the liver is extracting, in which case E_{liv} denotes the hepatic extraction ratio.

We identified two distinct phases in Fig. 3 (top): (i) an initial transient phase resulting from distributional processes; and (ii) a quasi-steady state elimination phase (approximately after 4 h, Fig. 3). Apparently, the "kinetic diversity" of concentration-time profiles is much smaller than the potential 13 dimensions of the PBPK model. We easily identify four different groups of organs and tissue with almost identical normalized concentration-time profiles: {muscle}, {adipose, bone}, {skin} and {rest = all remaining tissues and organs}. These four groups defined the lumped compartments of the reduced model for Lidocaine. Since the PBPK model was assumed to be linear, the grouping does not depend on the administered dose.

A slightly different scaling gave further insight about the elimination phase. In Fig. 3 (bottom), the concentration-time profiles of all 13 compartments of the detailed PBPK model were scaled according to $C_{\text{tis}}(t)/C_{\text{tis}}(t_{el})$, where the time t_{el} has been chosen to lie safely in the quasi-steady state elimination phase (we choose $t_{el} = 8$ h for Lidocaine).

This scaling showed more clearly the differences in the initial distributional phase and the identical decay in the elimination phase. It can alternatively be obtained from the first one by including into the scaling factor K_{tis} some factor SF_{tis}, such that $C_{\text{tis}}(t_{el}) = K_{\text{tis}} \cdot \text{SF}_{\text{tis}}$. This additional factor has a physiological interpretation: The normalized concentrations $C_{\text{tis}}(t)/K_{\text{tis}}$ correspond to the venous blood concentrations leaving the compartments (by definition of the tissue-to-blood partition coefficient). Figure 3 (top) shows that venous blood concentrations leaving the compartments are *not* identical in the elimination phase. Since the liver is continuously eliminating drug from the blood, there is a net loss of drug from each compartment as a result of the decreasing concentration in the perfusing blood. This net loss depends on both, physiological parameters (like blood flows and organ

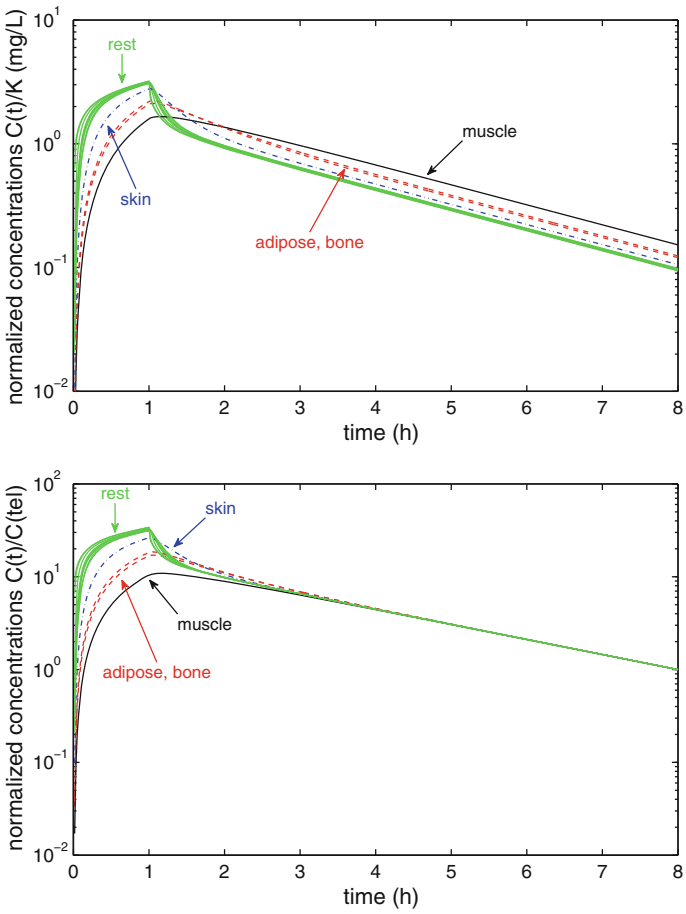

Fig. 3 Normalized tissue concentrations for Lidocaine based on predictions of the detailed, 13 compartment PBPK model. *Top*: Normalization of tissue concentrations C_{tis} based on the tissue-to-blood partition coefficient K_{tis} for non-eliminating tissues/organs, $K_{\text{liv}}(1 - \text{E}_{\text{hep}})$ for the liver. Vein and artery were not scaled. *Bottom*: Normalization of tissue concentrations C_{tis} based on the concentration $C_{\text{tis}}(t_{el})$ at some time t_{el} associated with the elimination phase (for non-eliminating tissues/organs and correspondingly for eliminating organs, artery and vein). We chose $t_{el} = 8$ h in this example. Identical colors/line styles indicate the proposed grouping of organs according to similar concentration-time profiles. Data correspond to an 60 min infusion of 400 mg Lidocaine. (Color figure online)

volumes), as well as drug-specific parameters, and is determining the additional factor SF_{tis}.

In summary, we used the normalized concentration-time profiles in Fig. 3 (top) to identify groups of compartments of the detailed PBPK model that behave kinetically similar. While we identified the organs to be lumped based on visual inspection, we also derived an automated procedure to identify organs with similar kinetics based on linear dependence of the normalized concentration-time profiles (see Appendix D).

Lumping condition

In accordance with Fig. 3, we derived the following

Lumping criteria:

$$\frac{C_1(t)}{K_1} = \frac{C_2(t)}{K_2} = \frac{C_{el}}{K_{el}(1 - \mathrm{E}_{el})} = \ldots, \tag{20}$$

where C_1, C_2 refer to non-eliminating compartments and C_{el} refers to, if any, an eliminating compartment (with extraction ratio E_{el}) to be lumped together. For Lidocaine, the only eliminating compartment was the liver. The lumping criteria allowed us to derive parameters and differential equations for the lumped compartment.

It is worth noticing that the above lumping criteria does not make any assumptions on whether organs or compartments are in series or parallel, as the previous lumping method by Nestorov et al. [11] did. We defined the central compartment ('cen') as the lumped compartment that contains the vein; and we denote the lumped compartment that contains the liver 'liv' as 'Liv'.

Parameter values for the lumped compartment

The volume of a lumped compartment V_{L} was defined as

$$V_{\mathrm{L}} = \sum_{\mathrm{tis}} V_{\mathrm{tis}}, \tag{21}$$

where the sum is taken over all original tissues/organs that were lumped. We defined the concentration C_{L} of the lumped compartment based on the conservation of mass as

$$C_{\mathrm{L}}(t) = \frac{1}{V_{\mathrm{L}}} \sum_{\mathrm{tis}} V_{\mathrm{tis}} C_{\mathrm{tis}}(t). \tag{22}$$

Exploiting the lumping criteria, and dividing the above equation by the blood concentration C_{blood} yielded the defining equation for the tissue-to-blood partition coefficient K_{L} for non-eliminating lumped compartments:

$$K_{\mathrm{L}} = \frac{1}{V_{\mathrm{L}}} \sum_{\mathrm{tis}} V_{\mathrm{tis}} K_{\mathrm{tis}}, \tag{23}$$

and for eliminating lumped compartments:

$$K_{\mathrm{Liv}} = \frac{1}{V_{\mathrm{Liv}}} \left(\sum_{\mathrm{tis} \neq \mathrm{liv}} V_{\mathrm{tis}} K_{\mathrm{tis}} + V_{\mathrm{liv}} K_{\mathrm{liv}} (1 - \mathrm{E}_{\mathrm{hep}}) \right), \tag{24}$$

where we formally defined $K_{\mathrm{ven}} = K_{\mathrm{art}} = 1$. For any lumped compartment except the central compartment, we defined the lumped blood flow Q_{L} by

$$Q_{\mathrm{L}} = \sum_{\mathrm{tis}} Q_{\mathrm{tis}}, \tag{25}$$

where the sum $\sum_{\mathrm{tis}}$ is taken over all original compartments that were lumped together into 'L'. The blood flow Q_{cen} of the central compartment was defined as

$$Q_{\mathrm{cen}} = \sum_{L} Q_{L}, \tag{26}$$

where the sum is taken over all lumped compartments that have an inflow into the central compartment.

Differential equations for the lumped compartments

We derived the equations for the rate of change of the concentration in the lumped compartment based on Eq. 22. The derivation is given in Appendix B. For each lumped compartment except the central compartment, it is

$$V_{\mathrm{L}} \frac{\mathrm{d}}{\mathrm{dt}} C_{\mathrm{L}} = Q_{\mathrm{L}} \left(\frac{C_{\mathrm{cen}}}{K_{\mathrm{cen}}} - \frac{C_{\mathrm{L}}}{K_{\mathrm{L}}} \right). \tag{27}$$

For the central compartment, we distinguished two situations. If the liver is part of the central compartment, then it is

$$V_{\mathrm{cen}} \frac{\mathrm{d}}{\mathrm{dt}} C_{\mathrm{cen}} = Q_{\mathrm{cen}} \left(C_{\mathrm{in}} - \frac{C_{\mathrm{cen}}}{K_{\mathrm{cen}}} \right) - \mathrm{CL}_{\mathrm{blood}} \frac{C_{\mathrm{cen}}}{K_{\mathrm{cen}}} + r_{\mathrm{iv,po(F_{,bio})}}, \tag{28}$$

where the inflowing concentration was given by

$$C_{\mathrm{in}} = \frac{1}{Q_{\mathrm{cen}}} \sum_{\mathrm{L}} Q_{\mathrm{L}} \frac{C_{\mathrm{L}}}{K_{\mathrm{L}}}, \tag{29}$$

and the sum is taken over all lumped compartments except the central compartment.

If the liver is not part of the central compartment, it is

$$V_{\mathrm{cen}} \frac{\mathrm{d}}{\mathrm{dt}} C_{\mathrm{cen}} = Q_{\mathrm{cen}} \left(C_{\mathrm{in}} - \frac{C_{\mathrm{cen}}}{K_{\mathrm{cen}}} \right) - \mathrm{CL}_{\mathrm{blood}} \frac{C_{\mathrm{Liv}}}{K_{\mathrm{Liv}}} + r_{\mathrm{iv}}, \tag{30}$$

while for the 'Liv' compartment it is

$$V_{\mathrm{Liv}} \frac{\mathrm{d}}{\mathrm{dt}} C_{\mathrm{Liv}} = Q_{\mathrm{Liv}} \left(\frac{C_{\mathrm{cen}}}{K_{\mathrm{cen}}} - \frac{C_{\mathrm{Liv}}}{K_{\mathrm{Liv}}} \right) + r_{\mathrm{po(F_{F\cdot G})}}. \tag{31}$$

The incoming concentration C_{in} in Eq. 30 is defined as in Eq. 29. Note the difference in the dosing term; while we used $F_{\mathrm{bio}} = (1 - \mathrm{E_{hep}})F_{\mathrm{F\cdot G}}$ in the dosing term of Eq. 28, we used $F_{\mathrm{F\cdot G}}$ in the dosing term of Eq. 31.

We remark that Eq. 28 is actually a special case of Eq. 30. In the latter case, the term $C_{\mathrm{Liv}}/K_{\mathrm{Liv}}$ corresponds to the concentration of the blood leaving the lumped compartment that contains the liver, which is identical to the blood concentration of the central compartment in the case, where the liver is lumped with the blood compartment according to Eqs. 32 and 35.

Prediction of individual tissue concentrations

Based on the lumping criteria, we could easily regain individual concentrations of the original compartments that were lumped together. This process amounts to reversing the lumping procedure. Based on the concentration C_L and partition coefficient K_L of the lumped compartment we determined the original tissue concentration by (see Appendix A for details)

$$C_{tis} = K_{tis} \cdot \frac{C_L}{K_L} \tag{32}$$

$$C_{vbL} = \frac{C_L}{K_L} \tag{33}$$

$$C_{liv} = K_{liv}(1 - E_{hep}) \cdot \frac{C_L}{K_L}, \tag{34}$$

where C_{vbL} denotes the venous concentration leaving the lumped compartment. If the liver is part of the central compartment, then $C_L/K_L = C_{cen}/K_{cen}$ in Eq. 34, otherwise it is $C_L/K_L = C_{Liv}/K_{Liv}$. For the venous blood, we have

$$C_{ven} = \frac{C_{cen}}{K_{cen}}. \tag{35}$$

It is important to notice that the scaled concentration C_{cen}/K_{cen} rather then C_{cen} itself is the venous blood concentration that is to be compared to experimental data. The blood concentration can be related to the plasma concentration $C_{plasma} = C_{ven}$/B:P using the blood-to-plasma partition coefficient B:P.

Step-by-step lumping procedure

In summary, the proposed lumping scheme comprised the following steps:

1. Simulate the whole-body PBPK model to predict the concentrations $C_{tis}(t)$ in all organs and tissues.
2. Plot the normalized concentrations according to Eq. 19 and identify the groups of organs/tissues with similar normalized concentration-time profiles.
3. For each group of organs/tissues L, determine the lumped volume, blood flow and partition coefficient according to Eqs. 21–26.
4. Use Eqs. 27–29 or Eqs. 29–31 to simulate the lumped model and to predict the lumped concentrations C_L for all groups of organs/tissues.
5. Use Eqs. 32–35 to predict the original tissue concentration C_{tis} from C_L for each organ/tissue group.

We have derived the lumped parameters and ODEs under the lumping condition. In practice, we require to hold it only approximately, i.e., we require only that the normalized concentrations are (very) close to each other, as it is also done in the existing lumping approaches.

Volume of distribution V_{ss}

The volume of distribution at steady state V_{ss} is defined as

$$V_{\mathrm{ss}} = \frac{A_{ss,\mathrm{tot}}}{C_{ss,\mathrm{ven}}}, \tag{36}$$

where $A_{ss,\mathrm{tot}}$ denotes the total amount of drug in the body and $C_{ss,\mathrm{ven}}$ the venous blood concentration in steady state. Noting that the tissue-to-blood partition coefficients K_{tis} are the ratios of the tissue and blood concentrations in steady state, and exploiting Eqs. 21, 22 and 24, we obtained

$$V_{\mathrm{ss}} = \sum_{L} V_L K_L \tag{37}$$

$$= V_{\mathrm{ven}} + V_{\mathrm{art}} + \sum_{\mathrm{tis}} V_{\mathrm{tis}} K_{\mathrm{tis}} + V_{\mathrm{liv}}(1 - \mathrm{E}_{\mathrm{hep}}) K_{\mathrm{liv}}, \tag{38}$$

where the first sum is taken over all compartments of the lumped model, and the second sum is taken over all non-eliminating tissues/organs of the detailed PBPK model. Hence, our lumping methods preserves the volume of distribution V_{ss}, which is identical to the volume of distribution of the original PBPK model (see Eq. 17). Importantly, preservation of V_{ss} does not depend on whether the eliminating liver organ is part of the central or any peripheral lumped compartment.

Relation to classical one- and two-compartment models

We compared our mechanistically lumped models with classical PK compartment models to obtain a potential mechanistic interpretation of classical models. We exemplified the relation for classical 1-compartment and 2-compartment models. We set $r_{\mathrm{admin}} = r_{\mathrm{iv,po}(\mathrm{F_{bio}})}$.

The mechanistic 1-compartment model was obtained by applying the lumping procedure to lump all compartments of the PBPK model into a single lumped compartment. The rate of change for the lumped concentration C_{cen} of the central compartment is given by

$$V_{\mathrm{cen}} \frac{\mathrm{d}}{\mathrm{dt}} C_{\mathrm{cen}} = r_{\mathrm{admin}} - \mathrm{CL}_{\mathrm{blood}} \frac{C_{\mathrm{cen}}}{K_{\mathrm{cen}}} \tag{39}$$

where V_{cen} denotes the total volume of all organs/tissues (defined as in Eq. 21), and K_{cen} denotes the tissue-to-blood partition coefficient for the central compartment (defined as in Eq. 24). The classical 1-compartment model was defined as

$$V_{\mathrm{ss}} \frac{\mathrm{d}}{\mathrm{dt}} C_1 = r_{\mathrm{admin}} - \mathrm{CL} \cdot C_1, \tag{40}$$

where V_{ss} denotes the volume of distribution, C_1 the total tissue concentration and CL the total body clearance. Figure 4a illustrates the mechanistic as well as classical

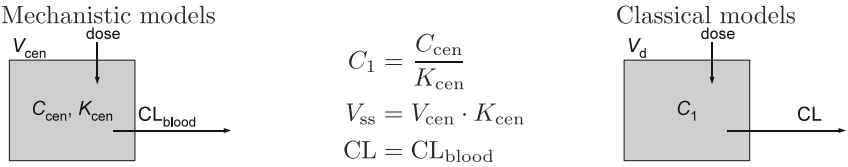

(a) Mechanistic vs. classical 1-compartment model. The corresponding ODEs are given in Eqs. 39 and 40. V_{cen} is identical to the total body volume.

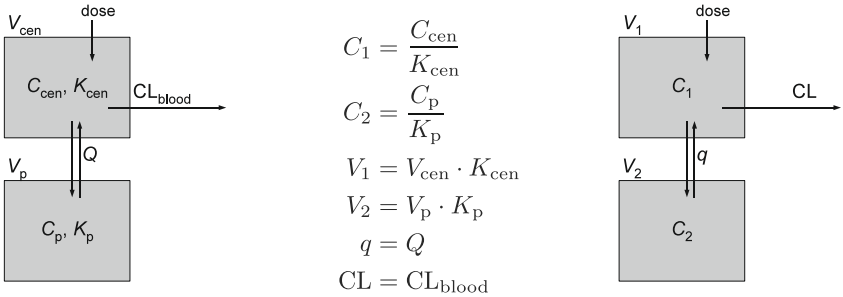

(b) Mechanistic vs. classical 2-compartment model. The corresponding ODEs are given in Eqs. 41–44. The sum of V_{cen} and V_p is identical to the total body volume.

Fig. 4 Relationship between mechanistic (*left*) and classical (*right*) 1 and 2-compartment models. The equations in the middle describe the relationship between the model parameters. The central compartment is by definition the lumped compartment containing the venous blood

1-compartment model, and shows the relationship between the model parameters (middle column).

The mechanistic 2-compartment model was derived under the assumption that the liver is part of the central compartment (alternative assignments are possible). The rate of change of the concentrations in the central and peripheral compartment C_{cen} and C_p with volumes V_{cen} and V_p and partition coefficients K_{cen} and K_p, respectively, were given by

$$V_{cen}\frac{d}{dt}C_{cen} = Q\left(\frac{C_p}{K_p} - \frac{C_{cen}}{K_{cen}}\right) - CL_{blood}\frac{C_{cen}}{K_{cen}} + r_{admin} \tag{41}$$

$$V_p\frac{d}{dt}C_p = Q\left(\frac{C_{cen}}{K_{cen}} - \frac{C_p}{K_p}\right) \tag{42}$$

Analogously, the classical 2-compartment model was specified in terms of the central and peripheral concentrations C_1 and C_2,

$$V_1\frac{d}{dt}C_1 = q \cdot C_2 - q \cdot C_1 - CL \cdot C_1 + r_{admin} \tag{43}$$

$$V_2\frac{d}{dt}C_2 = q \cdot C_1 - q \cdot C_2, \tag{44}$$

where V_1, V_2 denote the volumes of the central and peripheral compartment, respectively, q denotes the inter-compartmental transfer flow, and CL the hepatic

blood clearance. Figure 4(b) illustrates the mechanistic and classical 2-compartment models and the relationship between the model parameters.

Lumping of a 13 compartment whole-body PBPK model of perfusion rate-limited organs

We illustrated the proposed lumping approach for our model compound Lidocaine. The concentration-time profiles were clustered into four groups: {muscle}, {adipose, bone}, {skin}, and the central compartment containing all remaining organs {vein, artery, lung, brain, heart, kidney, gut, spleen, liver}. We used the different steps outlined in 'Step-by-step lumping procedure' to derive the corresponding set of ODEs.

The predicted concentration-time profiles for the different physiological compartments based on the lumped 4-compartment PK model and Eqs. 32–35 are shown in Fig. 2. All predicted organ/tissue concentrations were in excellent agreement with the predictions of the detailed 13-compartment PBPK model.

Lumping of a 18 compartment whole-body PBPK model of perfusion and permeability rate-limited organs

We used a detailed whole-body PBPK model for a homologous series of barbiturates in rats [11, 35] to illustrate application of our lumping method in the case, where some of the organs show permeability-limited distribution, while the remaining organs are perfusion rate-limited. The PBPK model comprised 18 organs, tissues and vascular compartments and is depicted schematically in Fig. 5. For all organs/tissues but brain and testes, a perfusion rate-limited, i.e, well-stirred, tissue model was assumed, whereas for brain and testes, tissue distribution was assumed to be permeability rate-limited. In addition to the liver metabolism, drug clearance of the unbound drug in plasma by the kidneys was taken into account. The required species- as well as drug-specific data were taken from [35]. For the tissue-to-unbound plasma partition coefficients, we used the optimized values reported in [35]. Simulation results for barbiturate C3 are shown in Fig. 7 (green solid line).

Figure 6 shows the normalized organ and tissue concentrations for all 18 compartments, where we included both, the vascular (vas) and the tissue (tis) concentration-time profiles for the two permeability rate-limited tissues testes and brain (as for plasma, we set the partition coefficients for the vascular parts of brain and testes to 1). We identified four sets of compartments to be lumped: {gut, spleen, pancreas, liver}, {skin, bone, brain(tis)}, {muscle, adipose, testes(tis)}, in addition to the central compartment {lung, artery, vein, kidneys, heart, stomach, brain(vas), testes(vas)}.

Our lumping approach naturally extends to permeability rate-limited organ models, as described in detail in Appendix C. For lumping of a permeability rate-limited organ, we derived the following

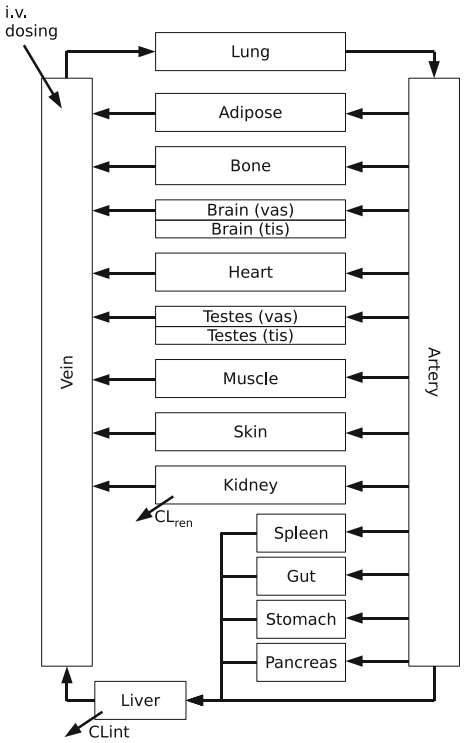

Fig. 5 Organ and tissue topology of the detailed, 18 compartment whole-body PBPK model for a barbiturate. Distribution in testes and brain was assumed to be permeability-rate limited, while it was assumed to be perfusion-rate limited for all remaining tissues and organs. The required species- as well as drug-specific data are given in [35]

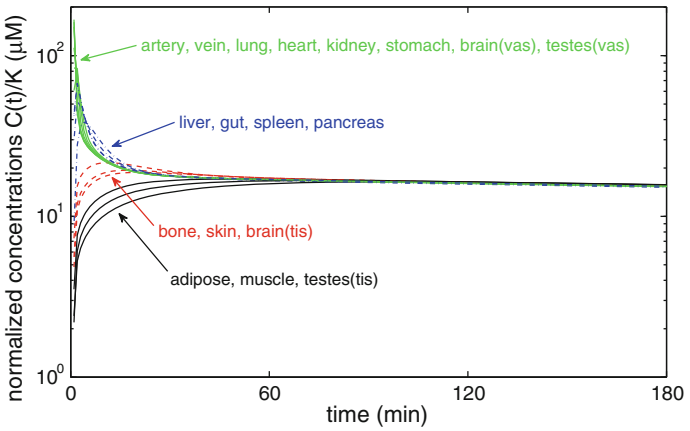

Fig. 6 Normalized tissue concentration for the barbiturate C3 based on predictions of an 18-compartment whole-body PBPK model [35]. Normalization based on the tissue-to-blood partition coefficient K_{tis} for non-eliminating tissues/organs, $K_{tis}(1 - E_{tis})$ for the two eliminating organs liver and kidney, and $C_{tis}(t)$ for the vein and the artery. Identical colors/line styles indicate the proposed lumping of organs according to similar concentration-time profiles. (Color figure online)

Permeability rate-limited criteria:

$$\frac{Q_{\text{tis}}}{\text{PS}_{\text{tis}} + Q_{\text{tis}}} > \frac{\text{PS}_{\text{tis}}}{\text{PS}_{\text{tis}} + Q_{\text{tis}}}. \tag{45}$$

This criteria ensures that permeability rather than perfusion is the rate-limiting step of tissue distribution. For details see Eq. 85. If this condition would be violated, then the model could reasonably be considered as either mixed perfusion and permeability rate-limited, or as solely perfusion rate-limited (depending on the actual values). In the former case, the interplay between vascular and tissue part is expected to be critical, such that the compartment should be left un-lumped. In the latter case, the organ model could be changed to the simpler perfusion rate-limited model. For the barbiturate C3, the permeability rate-limited criteria was satisfied for both, brain and testes.

Under the permeability rate-limited criteria, the vascular part of a permeability rate-limited organ can be lumped together with the venous blood, while the tissue parts are lumped based on (see Appendix Eq. 87)

$$V_{\text{tis}} \frac{\text{d}}{\text{dt}} C_{\text{tis}} = \frac{\text{PS}_{\text{tis}} \cdot \text{Q}_{\text{tis}}}{\text{PS}_{\text{tis}} + Q_{\text{tis}}} \cdot \left(C_{\text{blood}} - \frac{C_{\text{tis}}}{K_{\text{tis}}} \right). \tag{46}$$

Hence, when lumping the tissue part of a permeability-limited tissue model, the term

$$\frac{\text{PS}_{\text{tis}} \cdot \text{Q}_{\text{tis}}}{\text{PS}_{\text{tis}} + Q_{\text{tis}}} \tag{47}$$

takes the role of the tissue blood flow Q_{tis} for perfusion rate-limited models (cf. Eq. 25).

Predictions of the lumped 4-compartment model are shown in Fig. 7 (dashed black line) for different organs and tissues. For almost all of the organs/tissues, the predictions were in excellent agreement with the detailed 18 compartment model. For muscle and adipose, the initial concentrations were slightly overestimated. This could be improved by considering adipose as a separate compartment in the lumped model, which would then comprise 5 compartments.

Characteristic features of mechanistically lumped PK models for moderate-to-strong bases, weak bases, and acids

A major determinant of drug disposition is tissue distribution. We used a recent approach to a priori predict tissue-to-unbound plasma partition coefficients [15–18] to parameterize the 13-compartment whole-body PBPK model for a number of different drugs. These in silico approaches regard the tissue as comprising an interstitial and an intra-cellular space. The unbound drug is possibly ionized in the interstitial and intra-cellular space and the neutral species can cross membranes by passive diffusion. In the intra-cellular space, the neutral species may distribute into neutral lipids and neutral phospholipids. In addition, a drug may bind to further tissue constituents. For moderate-to-strong bases, it is assumed that binding to acidic phospholipids is a major determinant of intra-cellular distribution. For weak

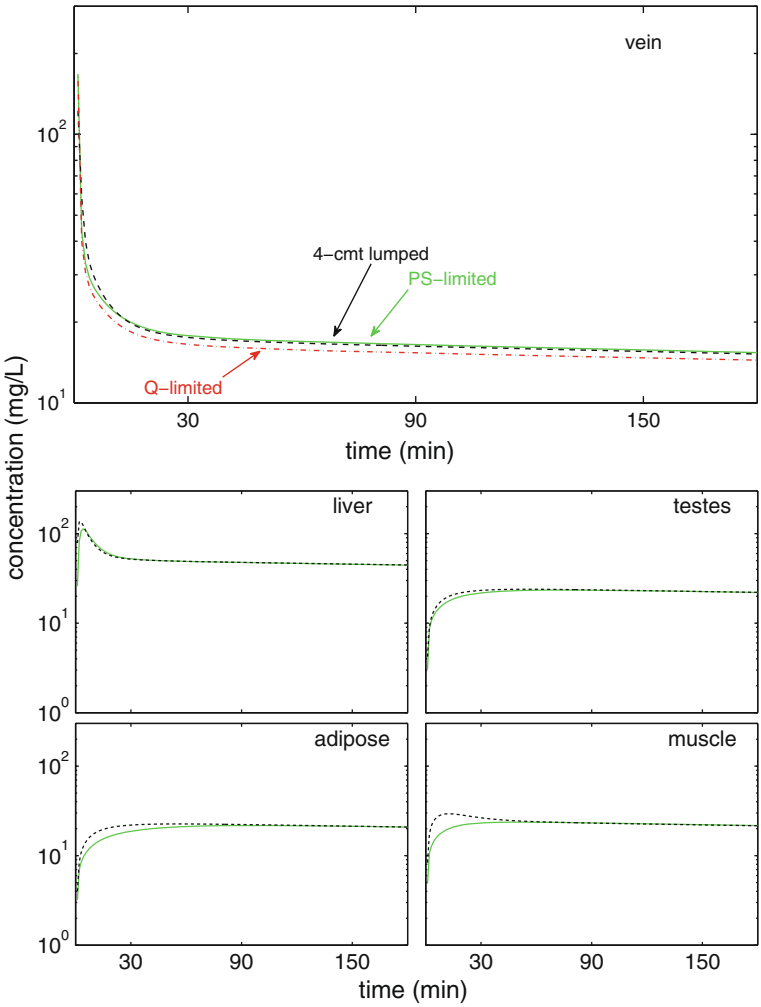

Fig. 7 Comparison of predictions of an 18 compartment whole-body PBPK model including permeability rate-limited compartments for brain and testes (*green solid line*, 'PS-limited') and our lumped 4-compartment PK model (*black dashed line*, '4-cmt lumped') following a 25 μmol i.v. bolus dose of a barbiturate C3 [35] in the rat for representative organs/tissues. The permeability rate-limited PBPK model and the lumped 4-compartment PK model show very good agreement for almost all compartments (see liver and testes for two out of 14). Adipose and muscle are slightly overestimated initially. For venous blood, predictions for an artificially transformed whole-body PBPK model, where the compartments brain and tested were converted to the perfusion rate-limited model, are shown (*red dot-dashed line*, 'Q-limited'). This model was the starting point of existing lumping methods, since they were not able to lump permeability rate-limited models. (Color figure online)

bases, neutrals and acids, binding in the interstitial space is an important determinant. It is assumed that weak bases and acids bind to albumin, while neutrals are assumed to bind to lipoproteins [15, 17, 36].

We investigated, whether mechanistically lumped PK models exhibit characteristic features based on the alkalinity/acidity of the drug. We considered 25 drugs with different alkalinity/acidity. See Table 3 for the drug-specific parameters. The compounds were chosen from [24, 25, 27]. We restricted our analysis to those compounds for which all parameters for the PBPK modelling were available in literature. The availability of the blood-to-plasma ratio B:P was the limiting factor restricting the choice of drugs.

For each drug, we predicted the concentration-time profiles based on the generic 13-compartment whole-body PBPK model shown in Fig. 1 for a 60 min i.v. infusion. Administration by infusion was chosen, since it did not require any additional parameter values as, e.g., the absorption rate constant for oral absorption. We determined the number of compartments for a mechanistically lumped PK compartment model based on the algorithm outlined in Appendix D. The predicted number of compartments for the different compound classes moderate-to-strong bases, weak bases and acids are shown in Fig. 8.

For all drugs except Midazolam and Thiopental, a maximal 4-compartment lumped PK model was sufficient to predict the drug PK in all 13 different physiological tissues/organs. If a lumped model comprised more than a single compartment, then adipose, bone, muscle and skin were typically not part of the central compartment (see Fig. 9). From these four tissues/organs, skin usually showed closest similarity to the central compartment.

In Table 2, physiological and anatomical data for adipose, bone, muscle and skin are listed for an average human. Their important role in tissue distribution is due to

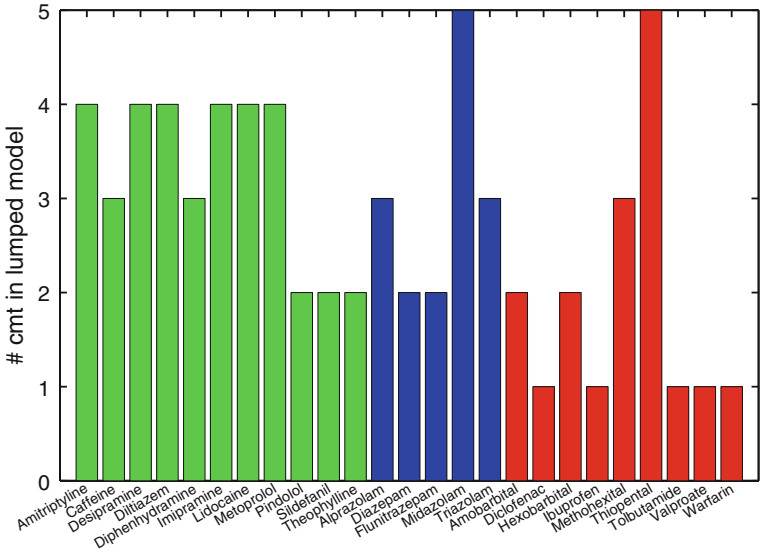

Fig. 8 Predicted number of compartments for the mechanistically lumped PK model based on concentration-time profiles generated by the 13-compartment whole-body PBPK models. The colors indicate the categorization of drugs as follows: moderate-to-strong bases (*left*, *green*), weak bases (*middle*, *blue*) and acids (*right*, *red*). (Color figure online)

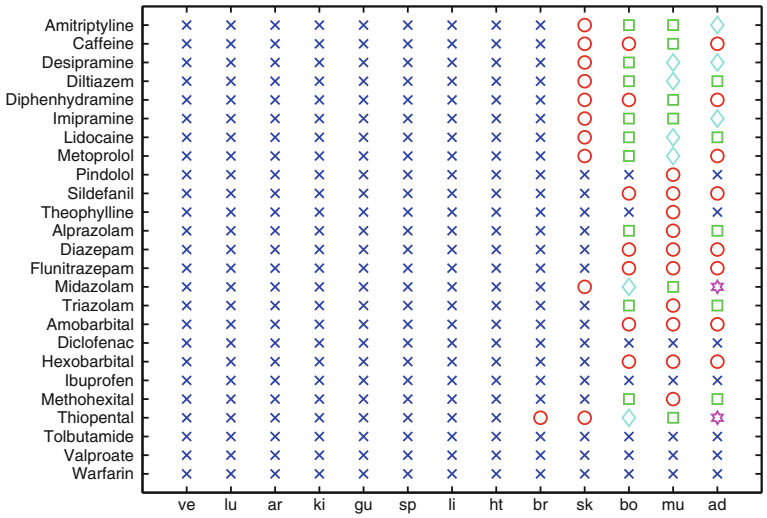

Fig. 9 Predicted assignment of organs, tissues and other spaces of the whole-body PBPK model to the lumped compartments of the mechanistically lumped model for the same 25 compounds as in Fig. 8. The central compartment is represented by x, potential additional peripheral compartments are represented by *circle*, *square*, *diamond* etc. The number of different symbols for a given compound corresponds to the number of compartments in the mechanistically lumped model

Table 2 Physiological and anatomical data for adipose, bone, muscle, skin and remaining tissues [6, 24]

	adipose	bone	muscle	skin	remaining organs
Volume	0.12	0.086	0.40	0.037	0.0026–0.026
Blood flows	0.05	0.05	0.17	0.05	0.02–1.0
Tissue water	0.15	0.44	0.76	0.62	0.72–0.81
Neutral lipids	0.79	0.074	0.024	0.028	0.003–0.051
Phospholipids	0.002	0.001	0.007	0.011	0.009–0.057

Volume: fraction of total body weight (BW); blood flow: fraction of cardiac output (co); tissue water, neutral lipids, phospholipds: fraction of total tissue volume (V_{tis}). The column 'remaining organs' lists the minimum and maximum value amongst all remaining organs considered in the whole-body PBPK model depicted in Fig. 1

their distinct characteristics. The four organs make the largest fraction of the total body volume with muscle being by far the largest tissue. At the same time, their blood flows are amongst the lowest. Regarding important tissue constituents influencing tissue distribution, the four tissues/organs typically show distinct characteristics at the extremes: adipose has lowest tissue water, high neutral lipids and low phospholipids; bone has lowest phospholipids, muscle and skin have high tissue water. These characteristics make them key tissues/organs in drug distribution.

For a number of acidic drugs, the predicted lumped compartment contained only a single compartment, while for other acids the number of compartments was 2, 3 or 5. We identified the fraction unbound in plasma fu^p as the discriminating parameter: For acids with a low fu^p (in our examples $fu^p \leq 0.1$) a mechanistically

1-compartment PK model was sufficient, while for acids with a moderate-to-high fu^p (in our examples $fu^p \geq 0.18$) two or more compartments were predicted.

For moderate-to-strong bases, muscle, bone, adipose, and skin were part of lumped compartments in different combinations. Mostly, muscle and skin formed separate compartments, if skin was not part of the central compartment (see Fig. 9).

Lumping and tissue distribution half-life

Based on the well-stirred tissue model, we may associate with each tissue a distributional half-life: Rearranging Eq. 1 yielded

$$\frac{\mathrm{d}}{\mathrm{dt}} C_{\mathrm{tis}} = \frac{Q_{\mathrm{tis}} C_{\mathrm{in}}}{V_{\mathrm{tis}}} - \frac{Q_{\mathrm{tis}}}{V_{\mathrm{tis}} K_{\mathrm{tis}}} \cdot C_{\mathrm{tis}}. \tag{48}$$

The pre-factor of the second summand can be interpreted as a distribution rate constant

$$k_{\mathrm{tis}} = \frac{Q_{\mathrm{tis}}}{V_{\mathrm{tis}} K_{\mathrm{tis}}} \tag{49}$$

associated with the tissue, where $V_{\mathrm{tis}} \cdot K_{\mathrm{tis}}$ can be understood as the volume of distribution associated with the tissue. For eliminating organs, K_{tis} was corrected by the tissue extraction ratio resulting in $K_{\mathrm{tis}}(1 - \mathrm{E}_{\mathrm{tis}})$. Based on k_{tis} we may characterize the kinetics of tissue distribution by the

$$\text{Tissue distribution half-life} = \frac{\ln(2)}{k_{\mathrm{tis}}}. \tag{50}$$

This half life corresponds to the situation, in which the inflowing drug concentration C_{in} is assumed to be constant. Tissue distribution is the slower the larger the product $V_{\mathrm{tis}} K_{\mathrm{tis}}(1 - \mathrm{E}_{\mathrm{tis}})$ or the smaller the blood flow Q_{tis} perfusing the tissue or organ.

In Fig. 10, the tissue distribution half-lives for the compounds listed in Table 3 are shown. Organs/tissues that were clustered together by our lumping method are marked with the same marker (cross, circle, square, etc). Noticeably, the tissue distribution half-life for different lumped compartments do not overlap. A decision on how to lump organs based on their tissue distribution half-life is possible—and the lumping criteria of existing lumping methods [11, 13]—but much harder.

Minimal lumped models as the link between PBPK and classical compartment models

The aim of the mechanistic lumping approach was to predict the concentration-time profiles of *all* organs and tissues from the lumped model. If only plasma or blood data are available, as is typically the case in clinical trials, the question arises whether it is possible to derive lumped PK compartment models that allow us to predict the venous blood concentration with as few compartments as possible. These models were termed 'minimal lumped models'. We used the predicted venous blood concentration by the 13-compartment whole-body PBPK model following a 400 mg i.v. infusion (60 min) of Lidocaine to illustrate minimal lumping.

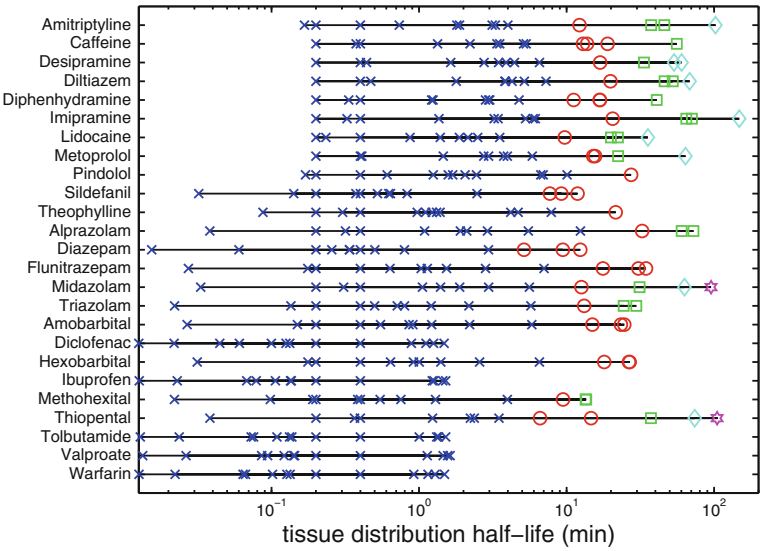

Fig. 10 Tissue distribution half-life for the same 25 compounds of Fig. 8 and all organs, tissues and other space of the generic 13-compartment PBPK model. For each compound, the 13 markers represent the 13 organs and tissues of the generic PBPK model. Identical symbols represent organs and tissues that were lumped together in our mechanistically lumped PK model. As in Fig. 9, the central compartment is represented by x, potential additional peripheral compartments are represented by *circle*, *square, diamond* etc. Artery (at 0.29 min) and vein (at 0.58 min) are clearly visible for all compounds, since these are the only two spaces whose half life does only depend on volume and blood flow, but not on a drug-specific partition coefficient

The minimal lumped model was determined on the basis of the mechanistically lumped model by further lumping together additional compartments. We started with a tentative minimal model comprising a {adipose, bone, muscle} compartment in addition to the central compartment and then moving further tissues into the central compartment. Predictions were checked against the detailed PBPK model predictions for the venous compartment.

Figure 11 shows the predicted blood concentrations of the mechanistically lumped 4-compartment PK model and a minimal lumped model in comparison to the prediction of the whole-body PBPK model. The minimal lumped model comprised a lumped compartment containing {adipose, bone, muscle} in addition to the central compartment. The parameter values of V_{cen}, V_p, Q and CL_{blood} are given in Table 4 (left). We inferred from Fig. 11 that predictions of the detailed PBPK model, the mechanistically lumped 4-compartment model, and the minimal 2-compartment model were almost identical for venous blood.

We further analyzed whether the minimal 2-compartment model could serve as a structural model to fit venous blood data generated by the whole-body PBPK model (considered as a surrogate for experimental data). The estimated parameters V_1, V_2, q and CL of the classical 2-compartment model are given in Table 4 (right), and the predicted concentration-time profile for venous plasma is shown in Fig. 11 (2-cmt emp. fit).

Table 3 Physicochemical and pharmacokinetic data of 25 diverse compounds

Drug	pK_a	log P_{ow}	fu^p	B:P	CL_{blood} (ml/min/kg)
Moderate-to-strong bases					
Amitriptyline	9.40[a]	4.90[a]	0.056[a]	0.86[a]	12.00[b]
Caffeine	10.40[a]	− 0.09[a]	0.700[a]	1.04[a]	1.40[c]
Desipramine	10.32[a]	4.90[a]	0.190[a]	0.96[a]	12.00[b]
Diltiazem	7.70[a]	2.67[a]	0.200[a]	1.03[a]	12.00[b]
Diphenhydramine	8.98[a]	3.31[a]	0.089[a]	0.80[a]	9.50[b]
Imipramine	9.50[a]	4.80[a]	0.130[a]	1.12[a]	12.00[b]
Lidocaine	8.01[a]	2.26[a]	0.296[a]	0.84[a]	15.00[c]
Metoprolol	9.70[a]	2.15[a]	0.900[a]	1.14[a]	12.15[c]
Pindolol	8.80[a]	1.75[a]	0.410[a]	0.81[a]	4.20[c]
Sildefanil	7.60[a]	2.75[a]	0.040[a]	0.62[a]	6.00[c]
Theophylline	8.71[a]	0.26[a]	0.600[a]	0.83[a]	0.65[c]
Weak bases					
Alprazolam	2.40[d]	2.09[d]	0.320[b]	0.78[b]	0.76[b]
Diazepam	3.38[d]	2.84[d]	0.013[b]	0.71[b]	0.60[b]
Flunitrazepam	1.80[d]	2.06[d]	0.250[e]	1.20[e]	9.8 (ml/min)[e]
Midazolam	6.01[d]	3.15[d]	0.050[b]	0.53[b]	8.70[b]
Triazolam	2.00[d]	2.42[d]	0.100[b]	0.62[b]	4.70[b]
Acids					
Amobarbital	7.90[d]	1.89[d]	0.390[b]	1.50[b]	0.35[b]
Diclofenac	4.15[f]	3.90[f]	0.005[b]	0.55[b]	7.60[b]
Hexobarbital	8.29[d]	1.74[d]	0.530[b]	1.00[b]	3.60[b]
Ibuprofen	4.70[d]	4.06[d]	0.010[b]	0.55[b]	1.50[b]
Methohexital	8.30[d]	1.72[d]	0.270[b]	0.70[b]	16.00[b]
Thiopental	7.53[d]	2.93[d]	0.180[d]	0.88[h]	2.02[i]
Tolbutamide	5.29[d]	2.39[d]	0.040[b]	0.55[b]	0.36[b]
Valproate	4.60[d]	2.76[d]	0.099[d]	0.55[j]	0.11[j]
Warfarin	5.08[g]	3.00[g]	0.010[b]	0.55[b]	0.081[b]

[a] [24], [b] [25], [c] [26], [d] [27], [e] [28], [f] [29], [g] [30], [h] [31], [i] [32], [j] [33]

Based on the relations given in Fig. 4, we determined the parameter values of V_1, V_2, q and CL from the minimal lumped model, see Table 4 (middle) for comparison. All parameters show excellent agreement.

We next studied minimal lumped models for the 25 model compounds in Table 3, see Fig. 12. Also here, the distinct role of the adipose, muscle and bone compartments was present. We used the residual error measure $\|\cdot\|_{PBPK}$ defined in Eq. 18 to quantify the difference between the venous plasma concentration predicted by the PBPK model and a potential minimal model, and regarded the minimal model as adequate, if the residual error was below $\varepsilon = 0.09$ (a common value for all drugs allowed for unbiased comparison).

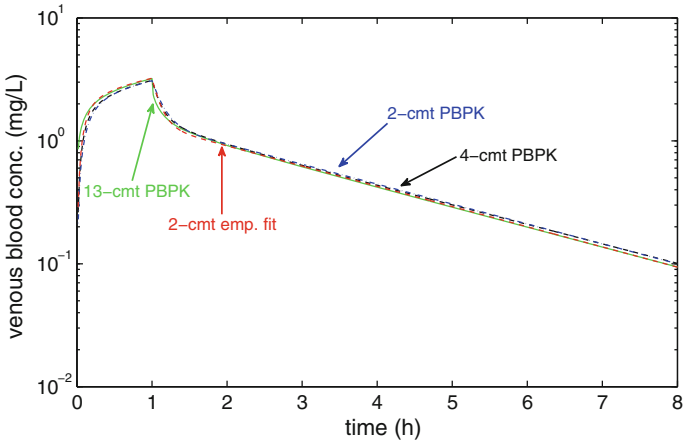

Fig. 11 Comparison of the 13-compartment whole-body PBPK model for Lidocaine to a mechanistically lumped 4-compartment model and a minimal lumped 2-compartment model for venous blood. In addition, the predictions of an empirically fitted classical 2-compartment model are shown. All models show excellent agreement

Table 4 Comparison of parameters of the fitted classical 2-compartment model (*right*) and the minimal lumped model (*left* and *middle*)

Minimal model		Determination of empiric parameters based on:		
			Minimal parameters	Empirical fitting
V_{cen}	14.33	V_1	29.7	21.5
V_p	44.18	V_2	99.1	99.8
Q	1.91	q	1.91	1.85
K_{cen}	2.07	CL	1.10	1.09
K_p	2.24			

Parameters of the minimal lumped model (*left*) were transformed into corresponding parameters of the classical compartment model as in Fig. 4 (*middle*)

For Midazolam and Thiopental, the minimal lumped model comprised 3 compartments. For those compounds where the mechanistically lumped model already comprised only 1- or 2-compartments, this number could not be further reduced. For all other compounds, a minimal 2-compartment model comprising an {adipose, muscle, bone} compartment in addition to the central compartment resulted in excellent predictions for venous plasma when compared to those predicted by the whole-body PBPK model.

Alternative routes of administration

In this section we analyzed the impact of the route of administration on mechanistically lumped and minimal lumped models.

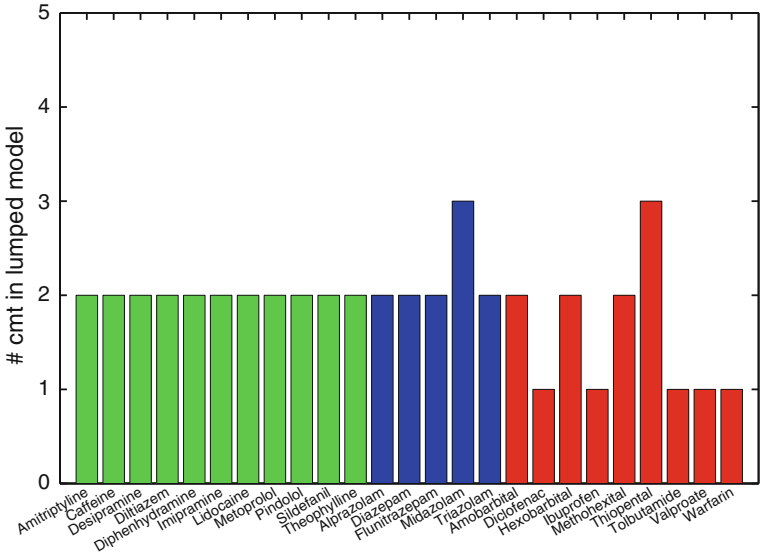

Fig. 12 Predicted number of compartments for the minimal lumped PK model based on concentration-time profiles generated by the 13-compartment whole-body PBPK models. The colors indicate the categorization of drugs as follows: moderate-to-strong bases (*left*, *green*), weak bases (*middle*, *blue*) and acids (*right*, *red*). (Color figure online)

Per oral administration

We used the detailed whole-body PBPK model to predict a single p.o. administration of 400 mg Lidocaine. We used $F_{\mathrm{F.G}} = 1$, and due to the absence of a human value the canine first order absorption rate constant $\lambda = 0.018$ min^{-1} [37]. After oral administration of Lidocaine in human, maximum plasma concentrations have been observed between 30 and 45 min [38], which is in accordance with the chosen absorption rate constant.

Figure 13 (top) shows the normalized concentrations $C_{\mathrm{tis}}/(K_{\mathrm{tis}}(1 - E_{\mathrm{tis}}))$. The situation was almost identical to the situation of an i.v. infusion (cf. Fig. 3), except that the normalized liver concentration showed a different 'shape'. This different shape is the result of the influx of drug through the portal vein. As a consequence, the number of compartments of the mechanistically lumped PK model increases by one: {muscle}, {adipose, bone}, {skin}, {liver} and {rest = all remaining tissues and organs}.

An increase in the number of compartments of the mechanistically lumped model does not necessarily result in an increased number of compartments of the minimal lumped model. Figure 13 (bottom) shows the venous plasma concentration as predicted by the 13-compartment whole-body PBPK model, the mechanistically lumped 5-compartment model, and a minimal lumped 2-compartment model comprising a {muscle, adipose, bone} compartment in addition to the central compartment. The predictions were in excellent agreement. Hence, although the p.o. administration increases the number of compartments of the mechanistically lumped

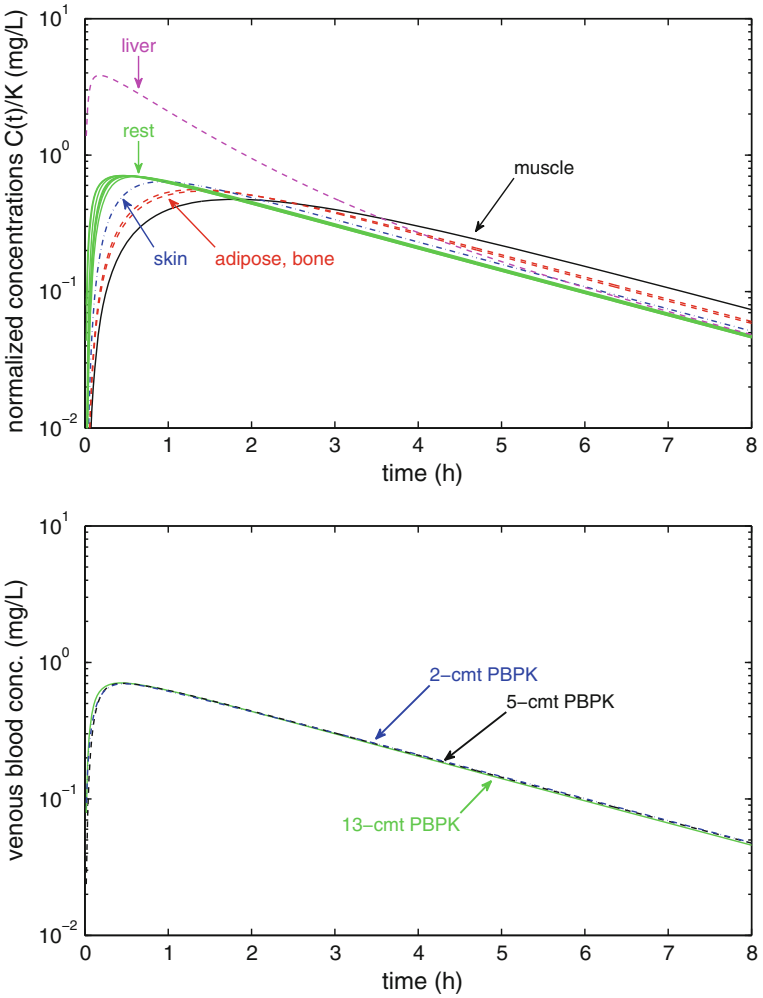

Fig. 13 Normalized tissue concentrations for Lidocaine based on predictions of the detailed, 13 compartment PBPK model for a p.o. administration. *Top*: Normalization of tissue concentrations C_{tis} based on the tissue-to-blood partition coefficient K_{tis} for non-eliminating tissues/organs, $K_{liv}(1 - E_{hep})$ for the liver. Vein and artery were not scaled. *Bottom*: Comparison of the 13-compartment whole-body PBPK model for Lidocaine to a mechanistically lumped 5-compartment model and a minimal lumped 2-compartment model for venous blood for p.o. administration. Data correspond to a single dose of 400 mg Lidocaine and show excellent agreement

compartment, it did not increase the number of compartments of the minimal lumped model.

Intravenous bolus administration

We next analyzed an i.v. bolus administration of 400 mg Lidocaine. Figure 14 (top) shows the normalized concentrations $C_{tis}/(K_{tis}(1 - E_{tis}))$. The number of distinct

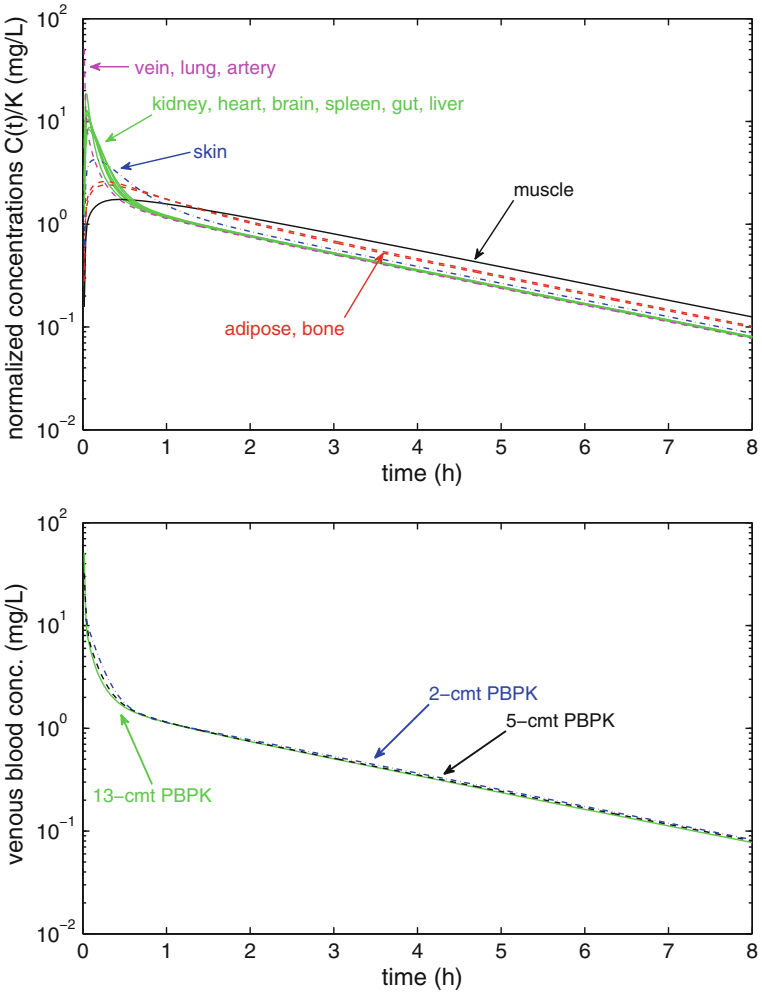

Fig. 14 Normalized tissue concentrations for Lidocaine based on predictions of the detailed, 13 compartment PBPK model for an i.v. bolus administration. *Top*: Normalization of tissue concentrations C_{tis} based on the tissue-to-blood partition coefficient K_{tis} for non-eliminating tissues/organs, $K_{liv}(1 - E_{hep})$ for the liver. Vein and artery were not scaled. *Bottom*: Comparison of the 13-compartment whole-body PBPK model for Lidocaine to a mechanistically lumped 5-compartment model and a minimal lumped 2-compartment model for venous blood for an i.v. bolus administration. Data correspond to a single dose of 400 mg Lidocaine and show excellent agreement

concentration-time profiles in comparison to the i.v. infusion (cf. Fig. 3) is again increased by one: {muscle}, {adipose, bone}, {skin}, {vein, lung, artery} and {rest = all remaining tissues and organs}. The mechanistically lumped model yielded excellent predictions for all organs from 10 min on. If concentration-time profiles below 10 min have to be predicted, then the number of compartments in the mechanistically lumped model would have to be increased to account for the very first distributional phase.

Figure 14 (bottom) shows the venous plasma concentration as predicted by the 13-compartment whole-body PBPK model, the mechanistically lumped 5-compartment model, and a minimal lumped 2-compartment model comprising a {muscle, adipose, bone} compartment in addition to the central compartment. Again, all predictions are in excellent agreement, and the number of compartments of the minimal lumped model was the same as for an i.v. bolus and an i.v. infusion administration.

Discussion

In this study we present a novel lumping method for the reduction of whole-body physiologically-based pharmacokinetic models. We used the proposed method to translate knowledge present in a 13- and 18-compartment PBPK model into mechanistically lumped 4-compartment and minimal 2-compartment models. The proposed method has several advantageous features: (i) there is no restriction on how organs and tissues can be lumped together; (ii) it is possible to lump perfusion rate-limited as well as permeability rate-limited compartment models; (iii) concentrations of the original compartments can be predicted based on the concentrations of the lumped model; and (iv) the lumping conditions have a physiological interpretation and are easily visualized. These are significant advancements over existing lumping methods [11–14].

Nestorov et al. [11] were the first to derive standard lumping principles for PBPK models. Their lumping principles are based on four conditions: (i) only organs can be lumped together that are either in parallel or in series (referring to the tissue topology in Fig. 1); (ii) permeability rate-limited models have to be approximated by perfusion rate-limited models as a pre-processing step; (iii) vein, lung and artery are either lumped together or left separate; and (iv) lumping of tissues is based on similar or small time constants. For non-eliminating tissues, this time constant is defined as

$$T_{\text{tis}} = \frac{V_{\text{tis}} \cdot K_{\text{tis}}}{Q_{\text{tis}}}, \tag{51}$$

while for eliminating organs it is

$$T_{\text{tis}} = \frac{V_{\text{tis}} \cdot K_{\text{tis}}}{Q_{\text{tis}} + \text{fu}_{\text{blood}}\text{CL}_{\text{int}}}, \tag{52}$$

where V_{tis}, Q_{tis} and K_{tis} refer to the tissue volume, the tissue blood flow and the tissue-to-blood partition coefficient, respectively; and fu_{blood} and CL_{int} denote the fraction unbound in blood and the intrinsic clearance, respectively. Thus, given the topology in Fig. 1, the smallest lumped model consistent with the above conditions (i)-(iii) has at least four lumped compartments: {vein, lung, artery}, {spleen, gut}, {liver}, {all other compartments}. While their equations for the lumped volume, blood flow and partition coefficient are identical to our Eqs. 21, 25 and 23, it is the lumping criterium (and thereon build derivations) that distinguishes our approach from the existing approaches. The herein proposed

lumping criterium, e.g., allows a justified application of lumping, where existing lumping criteria fail. As a results, we can easily justify the reduction of a 13 dimensional whole-body PBPK model to a single lumped compartment.

The detailed whole-body PBPK model for barbiturates was used by Nestorov et al. [11] to demonstrate their lumping approach. As an pre-processing step, however, the permeability rate-limited tissue distribution model for brain and testes had to be transformed into a perfusion-rate limited model [11]. This reduced the number of compartments to 16, eliminating the two vascular spaces of brain and testes. The simulation results of the artificially transformed PBPK model are shown in Fig. 7(a) (dot-dashed black line, 'Q-limited'). The differences of the predictions between the artificially transformed 16-compartment PBPK model and the original 18-compartment PBPK model are much larger than the difference between the predictions of our lumped 4-compartment model and the original PBPK model.

As in our approach, Nestorov et al. [11] lump together tissues with similar kinetics. Their measure of similarity is based on the time constant T_{tis} (Eqs. 51–52). Some rule of thumb on how similar the time constants T_{tis} have to be is given in [11, p. 32–33]. The time constant is related to the tissue distribution half-life by (cf. Eq. 50)

$$\text{Tissue distribution half-life} = \ln(2) \cdot T_{\text{tis}}. \tag{53}$$

Given a list of time constants (see Fig. 10 for a variety of compounds), it can be very difficult to decide which compartments to lump. Moreover, the time-constants are independent of any administration details and as such cannot predict different structures of lumped models for different administrations/dosing schemes. In our approach, the lumping condition is based on the transient feature of tissue distribution as well as on the elimination phase after distribution reached quasi-steady state.

The lumping method in [11, 13] does not relate the predictions of the lumped model back to predictions of the organs and tissues of the original whole-body PBPK model. Instead, for comparison with the predictions of the lumped model, the whole-body PBPK model predictions need to be lumped. The same applies to a comparison with experimental data. If experimental data were only available for one, but not all of the original compartments that comprise a lumped compartment, such an approach would not be applicable. As a consequence, Brochot et al. [12] introduced a constraint lumping approach, where some of original variables are left unlumped. While this solves the above mentioned problem, it increases the number of compartments of the lumped model. With our proposed lumping approach both aims, a small number of compartments of the lumped model as well as the possibility to predict original organ and tissue concentration-time profiles, can be achieved at the same time.

If we were only interested in predictions of the venous blood concentration (as part of the central compartment), then a further reduction is possible. For our model compound Lidocaine, we were able to further reduce the lumped 4-compartment model to a minimal lumped 2-compartment model. A further reduction to one compartment did seriously compromise the predictions for the central compartment,

as one would expect due to the bi-exponential characteristics of the concentration-time profiles.

Analyzing minimal models for a variety of compounds revealed that a minimal 2-compartment model comprising an {adipose, bone, muscle} compartment in addition to the central compartment (containing all remaining tissues) was almost always as good in predicting the *venous blood* concentration as the detailed PBPK model. This highlights and confirms the importance of adipose, bone and muscle tissue for drug distribution, which is due to their size and often distinct characteristics compared to the remaining organs/tissues (cf. also Table 2). A more thorough analysis about how to more systematically derive a minimal lumped model from a mechanistically lumped model is work in progress.

The presented analysis based on 25 compounds is a first step towards a more comprehensive understanding of minimal lumped compartment models. The limiting factor for the number of compounds considered is the availability of the blood-to-plasma ratio B:P. From the point of in silico modeling and simulation, this parameter is an important datum. While it is nowadays by default measured in the drug discovery phase, it seems rarely be reported in drug data bases.

An important part of classical modelling is to specify the structure of the classical compartment model. This includes specification of the number of compartments, its connections, whether processes are linear or non-linear etc. Another important question is whether elimination takes place in the central or in the peripheral compartment. This might not only impact convergence of the estimation process, but also influence pharmacokinetic characteristics like, e.g., the volume of distribution [39, 40]. Commonly, the 'elimination at the point of observation' assumption is made, while a compartmental model with peripheral elimination might give rise to a larger volume of distribution [40].

We observed that for all compounds analyzed in this study, the liver was part of the central compartment, an observation in favor of the 'elimination at the point of observation' assumption.

A minimal lumped model derived from a whole-body PBPK model evaluated against pre-clinical and early clinical data can be interpreted as extrapolating the current knowledge about the drug PK into the next phase. At the same time, a classical compartment model, e.g., developed as a structural model in population analysis of clinical trials, based on new experimental data might be interpreted as representing the minimal description of this new information in terms of a PK model. A comparison of both models, therefore, offers the possibility to compare the expectations based on translating previous insights and knowledge with the information content of new clinical data in form of the classical model. This is a consistency check of the new data against previous knowledge. In addition, since the parameters of the classical model have to be estimated based on the experimental data, the parameters of our minimal lumped compartment model can be used as initial values in the estimation process, addressing the critical question of how to chose initial conditions in the parameter estimation process.

Our proposed lumping method in its current form applies to the important class of linear PK models. Extension to include non-linear behavior seems possible. Saturable metabolism is likely to be includable based on a non-linear extraction

ratio. Incorporation of further non-linearities might be more difficult, and results might then become dose dependent. A more thorough analysis of lumping including non-linearities has to be left for the future.

Applying our lumping method to a diversity of drugs allowed us to obtain some general insight on the kinetic diversity and the number of lumped compartments for different classes of compounds. Our analysis is based on recent advances in a priori models for predicting tissue-to-unbound plasma partition coefficients [15, 17]. Rather than grouping drugs according to therapeutic indications, we grouped them according to their alkalinity/acidity. We find that for weak and moderate-to-strong bases and for acids with moderate to high fraction unbound, the mechanistically lumped model typically comprised three to four compartments. For acids with low fraction unbound, i.e., high plasma protein binding, the lumped model comprised only a single compartment. For acids, the fraction unbound in plasma is used to determine the albumin association constant in the model to a priori predict tissue-to-unbound plasma partition coefficients [17]. From this it follows that acids with low fu^p strongly bind to interstitial albumin. This might explain why a 1-compartment model was sufficient to predict the concentration-time profile of the drug in all organs and tissues as predicted by the 13-compartment whole-body PBPK.

A first comparison to published classical PK models for analyzing clinical data showed a good agreement between the number of compartments used and the number of compartments of our minimal lumped model. For Midazolam and Thiopental, 2- and 3-compartment models have been used [41–44], while we predicted a minimal 3-compartment PK model. For Valproate, a 1-compartment model is reported by [45, 46], which is in agreement with our predictions (see Fig. 8). For Tolbutamide, a 2-compartment model was used in [47], while we predicted a minimal 1-compartment model. For Lidocaine, a 2- as well as a 3-compartment model was reported in [3, 48], while we predict a minimal 2-compartment model. Such a comparison can only be preliminary, since it does not take into account two important facts: the sparsity of the experimental data, and the variability inherent in the patient cohort of clinical trials. The first fact might result in a lower number of compartments in the estimated classical model, while the second fact is likely to result in a larger number of compartments estimated for the classical model.

In summary, the presented lumping method is the first step towards a more comprehensive approach to translate knowledge and insight from pre-clinical and early clinical development—given in form of a whole-body PBPK model—into the development of classical compartment models. In this article, we focussed on the static parameter case, i.e., the case of an individuum (including the fictive mean individuum). The next step will have to consider variability of the type that is present in patient collectives of clinical trials. In this regard, the development of methods to generate in silico populations suitable for PBPK modeling [22, 49], and the development of a methodology to consider parametric variability [13] are expected to prove useful. This opens the possibility to extend the presented lumping method to analyze and incorporate covariates and their expected impact into the lumped model.

Acknowledgements The authors kindly acknowledge comments on the manuscript by Charlotte Kloft (Clinical Pharmacy, Martin-Luther-Universität Halle-Wittenberg/ Germany), Steve Kirkland (Hamilton Institute, NUIM/Ireland), Andreas Reichel (Bayer Schering Pharma) and Olaf Lichtenberger (Abbott). S.P. acknowledges financial support from the Graduate Research Training Program PharMetrX: Pharmacometrics and Computational Disease Modeling, Martin-Luther-Universität Halle-Wittenberg and Freie Universität Berlin, Germany (http://www.pharmacometrics.de).

Appendix A: Derivation of the relation between the lumped and the original concentrations

The relation between the concentrations of the lumped compartment and the comprised original compartments is given by Eq. 22:

$$C_{\mathrm{L}} = \frac{1}{V_{\mathrm{L}}} \sum_{\mathrm{tis}} V_{\mathrm{tis}} C_{\mathrm{tis}}. \tag{54}$$

The idea is to establish a link between the concentration C_{tis} of one of the original organs (or tissues) and the concentration C_{L} of the associated lumped compartment. Let us arbitrarily choose one organ (named 'ref'). Using the lumping criteria, we have $C_{\mathrm{tis}}/K_{\mathrm{tis}} = C_{\mathrm{ref}}/(K_{\mathrm{ref}}(1 - E_{\mathrm{ref}}))$ and thus $C_{\mathrm{tis}} = C_{\mathrm{ref}} K_{\mathrm{tis}}/(K_{\mathrm{ref}}(1 - E_{\mathrm{ref}}))$ for all tissue/organs lumped into 'L'. In combination with the above equation for C_{L} this yielded

$$C_{\mathrm{L}} = \frac{1}{V_{\mathrm{L}}} \sum_{\mathrm{tis}} V_{\mathrm{tis}} \frac{K_{\mathrm{tis}}}{K_{\mathrm{ref}}(1 - E_{\mathrm{ref}})} C_{\mathrm{ref}}, \tag{55}$$

or equivalently

$$C_{\mathrm{L}} = \frac{1}{V_{\mathrm{L}}} \sum_{\mathrm{tis}} V_{\mathrm{tis}} K_{\mathrm{tis}} \cdot \frac{C_{\mathrm{ref}}}{K_{\mathrm{ref}}(1 - E_{\mathrm{ref}})}. \tag{56}$$

Using the definition of K_{L} in Eq. 23 and 24 we obtain the desired relation:

$$\frac{C_{\mathrm{L}}}{K_{\mathrm{L}}} = \frac{C_{\mathrm{ref}}}{K_{\mathrm{ref}}(1 - E_{\mathrm{ref}})}. \tag{57}$$

Since the tissue/organ 'ref' was arbitrarily chosen, the above relation holds for every original compartment 'tis' that is part of the lumped compartment 'L', being eliminating (in which case $E_{\mathrm{ref}} > 0$) or non-eliminating (in which case $E_{\mathrm{ref}} = 0$).

Appendix B: General derivation of lumped ODEs

In the following, the subscript tis refers to all organs of the PBPK model excluding the liver, i.e., adi, bra, bon, gut, hea, kid, lun, mus, ski, spl.

To derive general equations for the rate of change of the lumped concentrations C_{L} it is advantageous to bring the original ODEs of the generic PBPK in a different but equivalent form, where elimination is associated with the venous compartment and all other compartments have the same structural form. In the generic PBPK

model (see Section 'Material and Methods'), the liver is assumed to be the only eliminating organ with ODE (see Eq. 3)

$$V_{\text{liv}} \frac{\text{d}}{\text{dt}} C_{\text{liv}} = Q_{\text{liv}} \cdot \left(C_{\text{in}} - \frac{C_{\text{liv}}}{K_{\text{liv}}} \right) - \text{CL}_{\text{int}} C_{\text{liv}}. \tag{58}$$

Defining $\text{R}_{\text{hep}} = \text{CL}_{\text{int}}\ K_{\text{liv}}/Q_{\text{liv}}$ and noting that $1 + \text{R}_{\text{hep}} = 1/(1 - \text{E}_{\text{hep}})$, where E_{hep} is the hepatic extraction ratio defined in Eq. 16, we obtain

$$V_{\text{liv}} \frac{\text{d}}{\text{dt}} C_{\text{liv}} = Q_{\text{liv}} \cdot \left(C_{\text{in}} - \frac{C_{\text{liv}}}{K_{\text{liv}}} \right) - Q_{\text{liv}} \text{R}_{\text{hep}} \frac{C_{\text{liv}}}{K_{\text{liv}}} \tag{59}$$

$$= Q_{\text{liv}} \cdot \left(C_{\text{in}} - (1 + \text{R}_{\text{hep}}) \frac{C_{\text{liv}}}{K_{\text{liv}}} \right) \tag{60}$$

$$= Q_{\text{liv}} \cdot \left(C_{\text{in}} - \frac{C_{\text{liv}}}{K_{\text{liv}}(1 - \text{E}_{\text{hep}})} \right). \tag{61}$$

Now, the inflowing concentration of the vein is given by (see Eq. 7)

$$C_{\text{in}} = \frac{1}{Q_{\text{co}}} \sum_{\text{tis}} Q_{\text{tis}} \frac{C_{\text{tis}}}{K_{\text{tis}}}, \tag{62}$$

which can be rewritten as

$$C_{\text{in}} = \frac{1}{Q_{\text{co}}} \left(\sum_{\text{tis} \neq \text{liv}} Q_{\text{tis}} \frac{C_{\text{tis}}}{K_{\text{tis}}} + Q_{\text{liv}} (1 - \text{E}_{\text{hep}}) \frac{C_{\text{liv}}}{K_{\text{liv}}(1 - \text{E}_{\text{hep}})} \right) \tag{63}$$

$$= \frac{1}{Q_{\text{co}}} \left(\sum_{\text{tis} \neq \text{liv}} Q_{\text{tis}} \frac{C_{\text{tis}}}{K_{\text{tis}}} + Q_{\text{liv}} \frac{C_{\text{liv}}}{K_{\text{liv}}(1 - \text{E}_{\text{hep}})} \right) - \frac{1}{Q_{\text{co}}} Q_{\text{liv}} \text{E}_{\text{hep}} \frac{C_{\text{liv}}}{K_{\text{liv}}(1 - \text{E}_{\text{hep}})}. \tag{64}$$

Let us define

$$\widehat{K}_{\text{tis}} = K_{\text{tis}}(1 - E_{\text{tis}}), \tag{65}$$

where E_{tis} denotes the tissue elimination ratio. In our case, it is $E_{\text{liv}} = \text{E}_{\text{hep}}$ and $E_{\text{tis}} = 0$ otherwise. Moreover, formally define $\widehat{K}_{\text{ven}} = \widehat{K}_{\text{art}} = 1$. Then, we finally obtain an equivalent formulation of the whole-body PBPK model. For all organs, tissues and other spaces except vein, it is

$$V_{\text{tis}} \frac{\text{d}}{\text{dt}} C_{\text{tis}} = Q_{\text{tis}} \cdot \left(C_{\text{in}} - \frac{C_{\text{tis}}}{\widehat{K}_{\text{tis}}} \right), \tag{66}$$

while for the vein it is

$$V_{\text{ven}} \frac{\mathrm{d}}{\mathrm{dt}} C_{\text{ven}} = Q_{\text{co}} \cdot \left(C_{\text{in}} - \frac{C_{\text{ven}}}{\widehat{K}_{\text{ven}}} \right) - \text{CL}_{\text{blood}} \frac{C_{\text{liv}}}{\widehat{K}_{\text{liv}}}, \tag{67}$$

where we exploit $\text{CL}_{\text{blood}} = Q_{\text{liv}} \text{E}_{\text{hep}}$ based on Eq. 67.

We determined the equation for the rate of change of the lumped concentration C_{L} by differentiating Eq. 22, yielding:

$$V_{\text{L}} \frac{\mathrm{d}}{\mathrm{dt}} C_{\text{L}} = \sum_{\text{tis}} V_{\text{tis}} \frac{\mathrm{d}}{\mathrm{dt}} C_{\text{tis}}. \tag{68}$$

The right hand side V_{tis}d/dt C_{tis} is defined in Eqs. 66 and 67. The right hand side of contain the concentrations of the original PBPK model C_{tis}, which can be determined using Eq. 57.

We obtained a very simple form of equations for the mechanistically lumped model, when spleen and gut were lumped together into the same compartment as the liver (hence they were part of the lumped 'Liv' compartment), and when lung and artery were lumped together into the same compartment as the vein (hence, they were part of the lumped 'cen' compartment). In this case, the influent concentrations will be identical for all compartments different from the central compartment. The rate of change for the concentration of the pre-lumped compartments spl-gut-liv ('sgl') and ven-lun-art ('vla') are

$$V_{\text{sgl}} \frac{\mathrm{d}}{\mathrm{dt}} C_{\text{sgl}} = Q_{\text{liv}} \left(C_{\text{art}} - \frac{C_{\text{liv}}}{\widehat{K}_{\text{liv}}} \right) \tag{69}$$

$$= Q_{\text{liv}} \left(C_{\text{art}} - \frac{C_{\text{sgl}}}{\widehat{K}_{\text{sgl}}} \right), \tag{70}$$

and

$$V_{\text{vla}} \frac{\mathrm{d}}{\mathrm{dt}} C_{\text{vla}} = Q_{\text{co}} \left(C_{\text{in}} - \frac{C_{\text{art}}}{\widehat{K}_{\text{art}}} \right) - \text{CL}_{\text{blood}} \frac{C_{\text{liv}}}{\widehat{K}_{\text{liv}}} \tag{71}$$

$$= Q_{\text{co}} \left(C_{\text{in}} - \frac{C_{\text{vla}}}{\widehat{K}_{\text{vla}}} \right) - \text{CL}_{\text{blood}} \frac{C_{\text{liv}}}{\widehat{K}_{\text{liv}}} \tag{72}$$

where C_{in} is the concentration flowing into the vein.

Now, we have for any lumped compartment excluding the central compartment:

$$V_{\text{L}} \frac{\mathrm{d}}{\mathrm{dt}} C_{\text{L}} = \sum_{\text{tis}} V_{\text{tis}} \frac{\mathrm{d}}{\mathrm{dt}} C_{\text{tis}} \tag{73}$$

$$= \sum_{\text{tis}} Q_{\text{tis}} C_{\text{art}} - \sum_{\text{tis}} Q_{\text{tis}} \frac{C_{\text{tis}}}{\widehat{K}_{\text{tis}}}, \tag{74}$$

where the sum is taken over all tissues that are lumped into 'L'. Our above assumption (resulting in Eq. 69) ensures that the inflowing concentration is the same

and identical to C_{art} for all tissue/organs. Exploiting the lumping condition $C_{\mathrm{tis}}/\widehat{K} = C_{\mathrm{L}}/K_{\mathrm{L}}$ yields

$$V_{\mathrm{L}}\frac{\mathrm{d}}{\mathrm{dt}}C_{\mathrm{L}} = \left(\sum_{\mathrm{tis}} Q_{\mathrm{tis}}\right)C_{\mathrm{in}} - \left(\sum_{\mathrm{tis}} Q_{\mathrm{tis}}\right)\frac{C_{\mathrm{L}}}{K_{\mathrm{L}}}. \tag{75}$$

Finally, using $Q_{\mathrm{L}} = \sum_{\mathrm{tis}} Q_{\mathrm{tis}}$ and $C_{\mathrm{art}} = C_{\mathrm{cen}}/K_{\mathrm{cen}}$ results in

$$V_{\mathrm{L}}\frac{\mathrm{d}}{\mathrm{dt}}C_{\mathrm{L}} = Q_{\mathrm{L}}\left(\frac{C_{\mathrm{cen}}}{K_{\mathrm{cen}}} - \frac{C_{\mathrm{L}}}{K_{\mathrm{L}}}\right). \tag{76}$$

For the central compartment, we obtain analogously

$$V_{\mathrm{cen}}\frac{\mathrm{d}}{\mathrm{dt}}C_{\mathrm{cen}} = Q_{\mathrm{cen}}\left(C_{\mathrm{in}} - \frac{C_{\mathrm{cen}}}{\widehat{K}_{\mathrm{cen}}}\right) - \mathrm{CL}_{\mathrm{blood}}\frac{C_{\mathrm{Liv}}}{K_{\mathrm{Liv}}}, \tag{77}$$

where we exploited the fact that $C_{\mathrm{liv}}/\widehat{K}_{\mathrm{liv}} = C_{\mathrm{Liv}}/K_{\mathrm{Liv}}$.

The above equations do not take into account any dosing. Again, as in the whole-body PBPK case, the corresponding ODEs of the lumped compartments comprising vein and liver have to be amended correspondingly. For an i.v. infusion r_{iv} (see Eq. 9 for the definition), it is

$$V_{\mathrm{cen}}\frac{\mathrm{d}}{\mathrm{dt}}C_{\mathrm{cen}} = Q_{\mathrm{cen}}\left(C_{\mathrm{in}} - \frac{C_{\mathrm{cen}}}{\widehat{K}_{\mathrm{cen}}}\right) - \mathrm{CL}_{\mathrm{blood}}\frac{C_{\mathrm{Liv}}}{K_{\mathrm{Liv}}} + r_{\mathrm{iv}}, \tag{78}$$

while for a p.o. administration $r_{\mathrm{po}(\mathrm{F}\cdot\mathrm{G})}$ (see Eq. 9 for the definition) it is

$$V_{\mathrm{Liv}}\frac{\mathrm{d}}{\mathrm{dt}}C_{\mathrm{Liv}} = Q_{\mathrm{Liv}}\left(\frac{C_{\mathrm{cen}}}{K_{\mathrm{cen}}} - \frac{C_{\mathrm{Liv}}}{K_{\mathrm{Liv}}}\right) + r_{\mathrm{po}(\mathrm{F}\cdot\mathrm{G})}. \tag{79}$$

If 'cen' and 'Liv' are identical, i.e., the liver is lumped into the central compartment, then it is $C_{\mathrm{cen}}/K_{\mathrm{cen}} = C_{\mathrm{Liv}}/K_{\mathrm{Liv}}$ and thus

$$V_{\mathrm{cen}}\frac{\mathrm{d}}{\mathrm{dt}}C_{\mathrm{cen}} = Q_{\mathrm{cen}}\left(C_{\mathrm{in}} - \frac{C_{\mathrm{cen}}}{\widehat{K}_{\mathrm{cen}}}\right) - \mathrm{CL}_{\mathrm{blood}}\frac{C_{\mathrm{cen}}}{K_{\mathrm{cen}}} + r_{\mathrm{iv,po}(\mathrm{F}_{\mathrm{bio}})}. \tag{80}$$

Note that in this case, the p.o. administration model has to account for the hepatic extraction, i.e., the absorption model with $F_{\mathrm{bio}} = (1 - \mathrm{E}_{\mathrm{hep}})F_{\mathrm{F}\cdot\mathrm{G}}$ (see Eq. 13) is used rather then the model with $F_{\mathrm{F}\cdot\mathrm{G}}$ (see Eq. 10).

Appendix C: Lumping of permeability rate-limited tissue model

The rates of change of the vascular concentration C_{vas} and the tissue concentration C_{tis} corresponding to a permeability limited tissue model are given by:

$$V_{\mathrm{vas}}\frac{\mathrm{d}}{\mathrm{dt}}C_{\mathrm{vas}} = Q_{\mathrm{tis}}\cdot(C_{\mathrm{in}} - C_{\mathrm{vas}}) - \mathrm{PS}_{\mathrm{tis}}\left(C_{\mathrm{vas}} - \frac{C_{\mathrm{tis}}}{K_{\mathrm{tis}}}\right) \tag{81}$$

$$V_{\mathrm{tis}}\frac{\mathrm{d}}{\mathrm{dt}}C_{\mathrm{tis}} = \mathrm{PS}_{\mathrm{tis}}\cdot\left(C_{\mathrm{vas}} - \frac{C_{\mathrm{tis}}}{K_{\mathrm{tis}}}\right). \tag{82}$$

The amount of drug that can transfer from the vascular to the tissue part is limited by the maximal amount of drug, entering the tissue, i.e, $Q_{\text{tis}}C_{\text{in}}$. This has to be taken into account, when lumping the tissue space together with other compartments. The following idea is similar to the approach to determine the blood clearance from the intrinsic clearance. It is based on a quasi-steady state assumption on C_{vas} (Eq. 81) yielding

$$0 = Q_{\text{tis}} \cdot (C_{\text{in}} - C_{\text{vas}}) - \text{PS}_{\text{tis}} \left(C_{\text{vas}} - \frac{C_{\text{tis}}}{K_{\text{tis}}} \right) \tag{83}$$

or

$$C_{\text{vas}} = \frac{Q_{\text{tis}}}{\text{PS}_{\text{tis}} + Q_{\text{tis}}} C_{\text{in}} + \frac{\text{PS}_{\text{tis}}}{\text{PS}_{\text{tis}} + Q_{\text{tis}}} \cdot \frac{C_{\text{tis}}}{K_{\text{tis}}}. \tag{84}$$

Thus, in steady state, the vascular concentration is a weighted sum of the influent concentration C_{in} and the concentration leaving the tissue compartment $C_{\text{tis}}/K_{\text{tis}}$. For permeability-rate limited organs, we would usually expect

$$\frac{Q_{\text{tis}}}{\text{PS}_{\text{tis}} + Q_{\text{tis}}} > \frac{\text{PS}_{\text{tis}}}{\text{PS}_{\text{tis}} + Q_{\text{tis}}}, \tag{85}$$

and as a consequence, we lump the vascular compartment with volume V_{vas} together with the blood compartment and approximate $C_{\text{vas}} = C_{\text{blood}}$.

Inserting this formula for C_{vas} into Eq. 82 for the tissue concentration yields

$$V_{\text{tis}} \frac{\text{d}}{\text{dt}} C_{\text{tis}} = \text{PS}_{\text{tis}} \cdot \left(\frac{Q_{\text{tis}} C_{\text{in}} + \text{PS}_{\text{tis}} \frac{C_{\text{tis}}}{K_{\text{tis}}}}{\text{PS}_{\text{tis}} + Q_{\text{tis}}} - \frac{C_{\text{tis}}}{K_{\text{tis}}} \right) \tag{86}$$

and finally

$$V_{\text{tis}} \frac{\text{d}}{\text{dt}} C_{\text{tis}} = \frac{\text{PS}_{\text{tis}} \cdot \text{Q}_{\text{tis}}}{\text{PS}_{\text{tis}} + Q_{\text{tis}}} \cdot \left(C_{\text{in}} - \frac{C_{\text{tis}}}{K_{\text{tis}}} \right). \tag{87}$$

Hence, when lumping the tissue part of a permeability-rate limited tissue model, the term

$$\frac{\text{PS}_{\text{tis}} \cdot \text{Q}_{\text{tis}}}{\text{PS}_{\text{tis}} + Q_{\text{tis}}} \tag{88}$$

should take the role of the tissue blood flow Q_{tis}. It is bounded by both Q_{tis} and PS_{tis}, as one would expect.

Appendix D: Automated determination of the number of lumped compartments of the mechanistically lumped model, and its composition

To compare the mechanistically lumped PK compartment models for a number of different drugs, we used an automated detection algorithm to determine the number of lumped compartment and its composition. The input were the normalized concentration-time profiles as predicted by the detailed whole-body PBPK model (cf. Eq. 19):

$$c_{\text{tis}}(t) = \frac{C_{\text{tis}}(t)}{K_{\text{tis}}(1 - E_{\text{tis}})}. \tag{89}$$

We determined the similarity matrix $M = (M_{ij})$ with entries

$$M_{i,j} = \frac{\langle c_{\text{tis}(i)}, c_{\text{tis}(j)} \rangle}{\langle c_{\text{tis}(i)}, c_{\text{tis}(i)} \rangle}, \tag{90}$$

where $\langle \cdot, \cdot \rangle$ denotes the Euclidian scalar product. In our setting, if C_{tis} is given as a vector at different time points $c_{\text{tis}}(t_1)$, ..., $c_{\text{tis}}(t_M)$ for some $M > 0$, then

$$\langle c_{\text{tis}(i)}, c_{\text{tis}(j)} \rangle \approx \sum_{k=1}^{M} c_{\text{tis}(i)}(t_k) \cdot c_{\text{tis}(j)}(t_k) \Delta t, \tag{91}$$

where we, for simplicity, assume that the time points are equally spaced with distance Δt.

Next, we determined the eigenvector v corresponding to the maximal eigenvalue of M. This eigenvector has an entry corresponding to each organ, tissue or other space of the whole-body PBPK model. We normalized the eigenvector

$$w(\text{tis}) = \frac{v(\text{tis})}{v(\text{ven})} \tag{92}$$

such that the normalized eigenvector satisfied $w(\text{ven}) = 1$. See Fig. 15 for the eigenvector corresponding to our model compound Lidocaine (for sake of illustration, we ordered the entries in increasing order).

We then considered the smallest entry of w (in the example corresponding to the muscle tissue) and lumped all organs that satisfied:

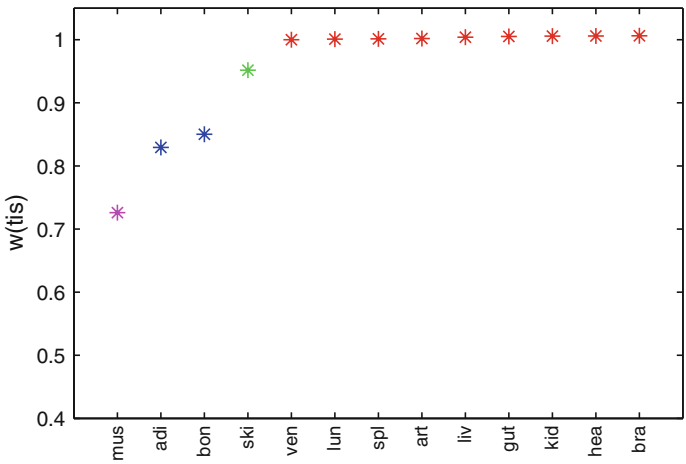

Fig. 15 Normalized eigenvector w corresponding to the maximal eigenvalue of the similarity matrix M based on the PBPK predictions of an 60 min i.v. infusion of 400 mg Lidocaine

$$w(\text{tis}) < w(\text{mus}) + \Delta w, \tag{93}$$

with $\Delta w = 0.045$. For our model compound Lidocaine, there was no such organ. Hence, the muscle tissue comprised a single lumped compartment. We proceeded with the next tissue (adipose in our example):

$$w(\text{tis}) < w(\text{adi}) + \Delta w. \tag{94}$$

In this case, w(bon) was the only organ to satisfy the above inequality so that adipose and bone were lumped together. We then proceeded with skin etc. The value of Δw was chosen so that the automated lumping procedure gave the same results as the manually chosen lumping for Lidocaine. The smaller the value of Δw the more similar the concentration-time profiles have to be for two organs/tissues to be lumped together.

For Caffeine, Diazepam and Amobarbital the predicted mechanistically lumped model was not sufficient to predict all concentration-time profiles of the 13-compartment whole-body PBPK model. In this case, we manually added a lumped compartment, which resolved the problem and increased the number of compartments by 1.

References

1. Kwon Y (2001) Handbook of essential pharmacokinetics, pharmacodynamics, and drug metabolism for industrial scientists. Springer-Verlag, New York, Inc
2. Derendorf H, Lesko LJ, Chaikin P, Colburn WA, Lee P, Miller R, Powell R, Rhodes G, Stanski D, Venitz J (2000) Pharmacokinetic/pharmacodynamic modeling in drug research and development. J Clin Pharmacol 40:1399–1418
3. Schoenwald RD (2002) Pharmacokinetics in drug discovery and development. CRC Press, Boca Raton
4. Tozer TN, Rowland M (2006) Introduction to pharmacokinetics and pharmacodynamics. Lippincott Williams & Wilkins, Philadelphia
5. Lüpfert C, Reichel A (2005) Development and application of physiologically based pharmacokinetic modeling toos to support drug discovery. Chem Biodivers 2:1462–1486
6. Jones HM, Parrott N, Jorga K, Lavé T (2006) A novel strategy for physiologically based predictions of human pharmacokinetics. Clin Pharmacokinet 45:511–542
7. Theil FP, Guentert TW, Haddad S, Poulin P (2003) Utility of physiologically based pharmacokinetic models to drug development and rational drug discovery candidate selection. Toxicol Lett 138:29–49
8. Schmitt W, Willmann S (2005) Physiology-based pharmacokinetic modeling: ready to be used. Drug Discov Today 2:125–132
9. Jones HM, Gardner IB, Watson KJ (2009) Modelling and PBPK simulation in drug discovery. AAPS J 11:155–166
10. Bourne DWA (1995) Mathematical modeling of pharmacokinetic data. Technomic Publishing Company, Inc., Lancaster
11. Nestorov IA, Aarons LJ, Arundel PA, Rowland M (1998) Lumping of whole-body physiologcally based pharmacokinetic models. J Pharmacokinet Pharmacodyn 26:21–46
12. Brochot C, Toth J, Bois FY (2005) Lumping in pharmacokinetics. J Pharmacokinet Pharmacodyn 32:719–736
13. Gueorguieva I, Nestorov IA, Rowland M (2006) Reducing whole body physiologically based pharmacokinetic models using global sensitivity analysis: diazepam case study. J Pharmacokinet Pharmacodyn 33:1–27

14. Björkman S (2003) Reduction and lumping of physiologically based pharmacokinetic models: prediction of the disposition of fentanyl and pethidine in human by successively simplified models. J Pharmacokinet Pharmacodyn 30:285–307
15. Rodgers T, Leahy D, Rowland M (2005) Physiologically based pharmacokinetic modeling 1: predicting the tissue distribution of moderate-to-strong bases. J Pharm Sci 94:1259–1276
16. Rodgers T, Leahy D, Rowland M (2007) Errata: Physiologically based pharmacokinetic modeling 1: predicting the tissue distribution of moderate-to-strong bases. J Pharm Sci 96:3151–3152
17. Rodgers T, Rowland M (2005) Physiologically based pharmacokinetic modelling 2: predicting the tissue distribution of acids, very weak bases, neutrals and zwitterions. J Pharm Sci 95:1238–1257
18. Rodgers T, Rowland M (2007) Errata: physiologically based pharmacokinetic modelling 2: predicting the tissue distribution of acids, very weak bases, neutrals and zwitterions. J Pharm Sci 96:3153–3154
19. Gerlowski LE, Jain RK (1983) Physiologically based pharmacokinetic modeling: principles and application. J Pharm Sci 72:1103–1127
20. Nestorov IA (2003) Whole body pharmacokinetic models. Clin Pharmacokinet 42:883–908
21. Luttringer O, Theil FP, Poulin P, Schmitt-Hoffmann AH, Guentert TW, Lavé T (2003) Physiologically based pharmacokinetic modelling of disposition of epiroprim in humans. J Pharm Sci 92:1990–2007
22. Willmann S, Höhn K, Edginton A, Sevestre M, Solodenko J, Weiss W, Lippert J, Schmitt W (2007) Development of a physiologically-based whole-body population model for assessing the influence of individual variability on the pharmacokinetics of drugs. J Pharmacokinet Pharmacodyn 34:401–431
23. International Commission on Radiological Protection (ICRP) (2002) Basic anatomical and physiological data for use in radiological protection: reference values. ICRP Publication 89
24. Poulin P, Theil FP (2009) Development of a novel method for predicting human volume of distribution at steady-state of basic drugs and comparative assessment with existing methods. J Pharm Sci 9999:1–29
25. Obach RS (1999) Prediction of human clearance of twenty-nine drugs from hepatic microsomal intrinsic clearance data: an examination of in vitro half-life approach and nonspecific binding to microsomes. Drug Metab Dispos 27:1350–1359
26. Riley RJ, McGinnity DF, Austin RP (2005) A unified model for predicting human hepatic, metabolic clearance from in vitro intrinsic clearance data in hepatocytes and microsomes. Drug Metab Dispos 33:1304–1311
27. Rodgers T, Rowland M (2007) Mechanistic approaches to volume of distribution predictions: understanding the process. Pharm Res 24:918–933
28. Jones HM, Houston JB (2004) Substrate depletion approach for determining in vitro metabolic clearance: time dependencies in hepatocyte and microsomal incubations. Drug Metab Dispos 32:973–982
29. DrugBank (2010) Diclofenac. http://drugbank.ca/drugs/DB00586
30. DrugBank (2010) Warfarin. http://www.drugbank.ca/drugs/DB00682
31. Jung D, Mayersohn M, Perrier D, Calkins J, Saunders R (1982) Thiopental disposition in lean and obese patients undergoing surgery. Anesthesiology 56:269–274
32. Russo H, Simon N, Duboin MP, Urien S (1997) Population pharmacokinetics of high-dose thiopental in patients with cerebral injuries. Clin Pharmacol Ther 62:15–20
33. Löscher W (1978) Serum protein binding and pharmacokinetics of valproate in man, dog, rat and mouse. J Pharmacol Exp Ther 204:255–261
34. Food and Drug Administration (2004) Approval letter: Lidocaine
35. Blakey GE, Nestorov IA, Arundel PA, Aarons LJ, Rowland M (1997) Quantitative structure pharmacokinetics relationship I: development of a whole-body physiologically based pharmacokinetic model to characterize changes in pharmacokinetics across a homologous series of barbiturates in the rat. J Pharmacokinet Biopharm 25:277–312
36. von Kleist M, Huisinga W (2007) Physiologically based pharmacokinetic modelling: a sub-compartmentalized model of tissue distribution. J Pharmacokinet Pharmacodyn 34:789–806
37. Boyes RN, Adams HJ, Duce BR (1970) Oral absorption and disposition kinetics of lidocaine hydrochloride in dogs. J Pharmacol Exp Ther 174:1–8
38. Adjepon-Yamoah KK, Scott DB, Prescott LF (1974) The effect of atropine on the oral absorption of lidocaine in man. Eur J Clin Pharmacol 7:397–400
39. Berezhkovskiy LM (2004) Volume of distribution at steady state for a linear pharmacokinetic system with peripheral elimination. J Pharm Sci 93:1628–1640

40. Yates JWT, Arundel PA (2008) On the volume of distribution at steady state and its relationship with two-compartmental models. J Pharm Sci 97:111–122
41. Heizmann P, Eckert M, Ziegler WH (1983) Pharmacokinetics and bioavailability of midazolam in man. Br J Clin Pharmacol 16:43–49
42. Zomorodi K, Donner A, Somma J, Barr J, Sladen R, Ramsay J, Geller E, Shafer SL (1998) Population pharmacodynamics of midazolam administered by target controlled infusion for sedation following coronary artery bypass grafting. Anesthesiology 89:1418–1429
43. Swart EL, Zuideveld KP, de Jongh J, Danhof M, Thijs LG, van Schijndel RMJS (2003) Comparative population pharmacokinetics of lorazepam and midazolam during long-term continuous infusion in critically ill patients. Br J Clin Pharmacol 57:135–145
44. Stanski DR, Maitre PO (1990) Population pharmacokinetics and pharmacodynamics of thiopental: the effect of age revisited. Anesthesiology 72:399–402
45. Gugler R, Schell A, Eichelbaum M, Fröscher W, Schulz HU (1977) Disposition of valproic acid in man. Eur J Clin Pharmacol 12:125–132
46. Blanco-Serrano B, Otero MJ, Santos-Buelga D, Garcia-Sanchez MJ, Serrano J, Dominguez-Gil A (1999) Population estimation of valproic acid clearance in adult patients using routine clinical pharmacokinetic data. Biopharm Drug Dispos 20:233–240
47. Rostami-Hodjegan A, Peacey SR, George E, Heller SR, Tucker GT (1998) Population-based modeling to demonstrate extrapancreatic effects of tolbutamide. Am J Physiol Endocrinol Metab 274:758–771
48. Kwa A, Sprung J, Van Guilder M, Jelliffe RW (2008) A population pharmacokinetic model of epidural lidocaine in geriatric patients: effects of low-dose dopamine. Ther Drug Monit 30:379–389
49. Price PS, Conolly RB, Chaisson CF, Gross EA, Young JS, Mathis ET, Tedder DR (2003) Modeling interindividual variation in physiological factors used in PBPK models of humans. Crit Rev Toxicol 33:469–503